

Remarks on the penguin decay $B_s \rightarrow \phi\phi$ with prospects for FCCee

R. Aleksan ^a and L. Oliver ^b

^a IRFU, CEA, Université Paris-Saclay, 91191 Gif-sur-Yvette Cedex, France

^b IJCLab, Pôle Théorie, CNRS/IN2P3 et Université Paris-Saclay

bât. 210, 91405 Orsay, France

Abstract

We underline the theoretical interest of the vector-vector penguin decay $B_s \rightarrow \phi\phi$, very clean from the experimental point of view. The CP-violation asymmetry A_{CP}^{mix} comes from the interference of mixing and decay $\lambda_{\phi\phi} = \frac{q}{p} \frac{\bar{A}}{A}$. In the Standard Model (SM) and in the Naive Factorization limit, the CP phase from the mixing $\frac{q}{p}$ exactly cancels the CP phase from the decay ratio $\frac{\bar{A}}{A}$. Therefore, this mode is suitable to look for possible New Physics (NP) because A_{CP}^{mix} would directly indicate the departure from the SM in mixing. We estimate the deviation from this cancellation by analyzing possible small effects in the SM, using in particular the QCD Factorization scheme. We compare the theoretical expectation for A_{CP}^{mix} to the measurement of LHCb, and the implications for NP. We pay also special attention to the transverse amplitude $h = -$, the longitudinal and transverse polarization fractions, and the interesting helicity-dependent observables $\lambda_{\phi\phi}^{h=0}$ and $\lambda_{\phi\phi}^{h=-}$. On the other hand, we make an estimation of the expected sensitivity at the future FCCee experiment for the CP phase and modulus of $\lambda_{\phi\phi}$. We find $\delta(|\lambda_{\phi\phi}|) = 0.004$ and $\delta(\phi_{\phi\phi}) = 0.009$ rad and, comparing to the LHCb data, we point out the expectations at FCCee in the search of NP.

1 Introduction

The physics of B meson decays into two vector mesons is very rich due to the polarization degrees of freedom. In this paper we consider the Penguin decay $B_s \rightarrow \phi\phi$ that has been already experimentally studied at LHCb [1]. This mode is very clean since the final state includes two narrow resonances producing alto-

gether four charged kaons, which offers a clean experimental signature with very low background, provided the detector includes a good Particle Identification system.

On the other hand, this decay of a heavy meson into two light mesons is rather well understood in the SM within the QCD Factorization (QCDF) scheme.

We will here concentrate on two main kinds of observables, namely the polarization fractions, and the CP asymmetries in the interference between mixing and decay,

$$\lambda_{\phi\phi} = \left(\frac{q}{p}\right)_{B_s} \frac{A(\bar{B}_s \rightarrow \phi\phi)}{A(B_s \rightarrow \phi\phi)} \quad (1)$$

that occur in the time-dependent decay, in particular $A_{CP}^{mix} \simeq \text{Im}\lambda_{\phi\phi}$.

In Section 2 we describe the puzzle of the polarization fractions in Penguin decays like $\bar{B}_s \rightarrow \phi\phi$, as compared to tree decays. In Section 3 we describe the time-dependent decay of $B_s \rightarrow \phi\phi$, underlying the interesting observables and pointing out the result $A_{CP}^{mix} = 0$ with top dominance in mixing and Naive Factorization in decay. In Section 4, we estimate the deviations from this naive result by analyzing possible small effects, e.g. the contribution of other quarks in the box diagram and corrections of $O(\Gamma_{12}/M_{12})$ to mixing, and the ratio of decay amplitudes \bar{A}/A beyond Naive Factorization (NF) within the QCDF scheme applied to B meson decays into two light vector mesons [2, 3, 4, 5]. We gather the calculations for $B_s \rightarrow \phi\phi$ and give an estimation of A_{CP}^{mix} , to see by how much it differs from its vanishing in the NF calculation. In Section 5 we compare to the LHCb data and its implications for the search of New Physics (NP) in $B_s - \bar{B}_s$ mixing. In Section 6 we estimate the expected sensitivity of FCCee for the modulus and phase of $\lambda_{\phi\phi}$ and the implications for NP. In Section 7 we further comment in detail on the polarization-dependent rates and CP violation in the QCDF scheme. Finally, in Section 8 we make some caution remarks, and we conclude. In the Appendices we give useful formulas on the Wilson expansion (Appendix A), on the transverse $h = -$ amplitude (Appendix B) and on the annihilation for the longitudinal $h = 0$ amplitude within QCDF (Appendix C).

2 Polarization fractions for the decay $\bar{B}_s \rightarrow \phi\phi$

To be definite, let us write down the helicity amplitudes

$$\bar{A}_L = A[\bar{B} \rightarrow V_1(0)V_2(0)] , \quad \bar{A}_\pm = A[\bar{B} \rightarrow V_1(\pm)V_2(\pm)] \quad (2)$$

where V_1 and V_2 are respectively the emitted and the produced vector mesons.

Then the transversity amplitudes read

$$\bar{A}_{\parallel} = \frac{1}{\sqrt{2}}(\bar{A}_+ + \bar{A}_-), \quad \bar{A}_{\perp} = \frac{1}{\sqrt{2}}(\bar{A}_+ - \bar{A}_-) \quad (3)$$

with the corresponding transversity rate fractions f_L, f_{\parallel} and f_{\perp} , satisfying $f_L + f_{\parallel} + f_{\perp} = 1$.

Since the final quark is dominantly left-handed because of the $V - A$ structure of the Standard Model (SM), heavy quark symmetry implies the hierarchy

$$\bar{A}_L : \bar{A}_- : \bar{A}_+ = 1 : \frac{\Lambda_{QCD}}{m_b} : \left(\frac{\Lambda_{QCD}}{m_b}\right)^2 \quad (4)$$

As underlined in detail by Beneke et al. [3], the transverse amplitude \bar{A}_- is suppressed by a factor m_{V_2}/m_B relative to \bar{A}_L , and the axial and vector contributions to \bar{A}_+ cancel in the heavy quark limit, implying the hierarchy (4).

The limit

$$\bar{A}_+ = 0 \quad (5)$$

implies [3],

$$f_{\parallel} = f_{\perp} \quad (6)$$

The hierarchy (4) points out to

$$f_{\parallel} \simeq f_{\perp} \ll f_L \quad (7)$$

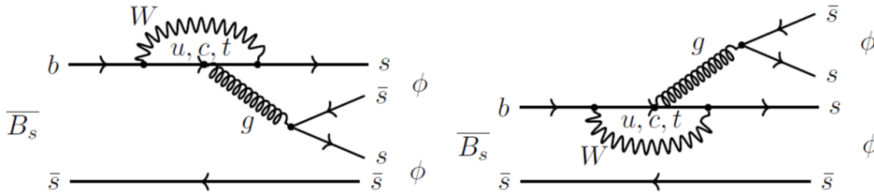


Fig. 1. A few perturbative diagrams contributing to the decay $B_s \rightarrow \phi\phi$, where g denotes one or several gluons with the right quantum numbers.

The decay mode $B_s \rightarrow \phi\phi$ is a penguin mode, as shown in Fig. 1 in terms of perturbative diagrams, and in Fig. 2 in terms of local Wilson Penguin operators.

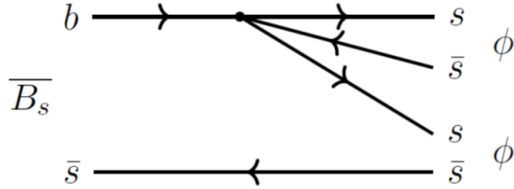


Fig. 2. One diagram in terms of local Wilson Penguin operators $O_i^{Penguin}$ contributing to the decay $B_s \rightarrow \phi\phi$.

It is very important to underline that the data for penguin-dominated B decays are in conflict with the expected hierarchy (7) [6, 7, 8] if one uses Naive Factorization, that predicts a large longitudinal fraction $f_L \sim 1$, in consistency with the data for tree decay modes, e.g. $\bar{B}_d \rightarrow \rho\rho$. We illustrate this point with the polarization data for $B_s \rightarrow \phi\phi$ [1] in Table 1.

Decay mode	BR ($\times 10^{-6}$)	f_L	f_{\parallel}	f_{\perp}
$\bar{B}_s \rightarrow \phi\phi$	18.5 ± 1.7	0.38 ± 0.01		0.29 ± 0.01

Table 1. Data on the rate and polarization fractions for the decay mode $\bar{B}_s \rightarrow \phi\phi$.

Among the Penguin transitions, $\bar{B}_s \rightarrow \phi\phi$ appears as a privileged mode, since one has for it a wealth of data, f_L, f_{\perp} and from Table 1 and the normalization condition, one gets $f_{\parallel} = 0.33 \pm 0.02$, that is rather precisely determined and consistent within errors with f_{\perp} , in agreement with the expectation following from (4,7). Also, $\bar{B}_s \rightarrow \phi\phi$ being a decay of the heavy meson into two light mesons, the theoretical QCDF framework applies.

The QCDF scheme includes NLO non-factorizable corrections of $O(\alpha_s)$, and the corresponding *effective* Wilson coefficients a_i^h are *helicity-dependent*. One could then expect that QCDF could eventually explain the gap between the data of Table 1 and the naive hierarchy (7). This is indeed the trend, as has been shown by the pioneering papers of Kagan [2], Beneke et al. [3] and Cheng and Yang [4].

For the particular case $\bar{B}_s \rightarrow \phi\phi$, we expose the main lines of the QCDF calculation of the polarization fractions in Section 7 and Appendices B, C where, following the papers by Beneke et al. [3] and by Bartsch et al. [5], we confirm the quantitative agreement with the experimental polarization fractions and rate. We also use below QCDF for the calculation of the time-dependent CP violation [5].

3 Time-dependent CP asymmetries in $\bar{B}_s \rightarrow \phi\phi$

For a decay of \bar{B}_s into a final state f , the time-dependent rate reads, up to small terms of $O(\Gamma_{12}/M_{12})$ [9],

$$\Gamma(\bar{B}_s(t) \rightarrow f) = |A_f|^2 \frac{1 + |\lambda_f|^2}{2} e^{-\Gamma t} \times \left[\cosh \frac{\Delta\Gamma t}{2} - A_{CP}^{dir} \cos(\Delta m t) + A_{\Delta\Gamma} \sinh \frac{\Delta\Gamma t}{2} - A_{CP}^{mix} \sin(\Delta m t) \right] \quad (8)$$

and for the case $\Gamma(B_s(t) \rightarrow f)$ the sign changes in front of the $A_{CP}^{dir}, A_{CP}^{mix}$ terms.

In (8), $\Delta m = m_H - m_L$ is the mass difference between the B_s eigenstates (H, L stand for heavy and light states), $\Gamma = \frac{\Gamma_H + \Gamma_L}{2}$, $\Delta\Gamma = \Gamma_L - \Gamma_H$ and A_f is the decay amplitude for $B_s \rightarrow f$. One has the coefficients

$$A_{CP}^{dir} = \frac{1 - |\lambda_f|^2}{1 + |\lambda_f|^2}, \quad A_{CP}^{mix} = -\frac{2 \operatorname{Im}\lambda_f}{1 + |\lambda_f|^2}, \quad A_{\Delta\Gamma} = -\frac{2 \operatorname{Re}\lambda_f}{1 + |\lambda_f|^2} \quad (9)$$

that satisfy $|A_{CP}^{dir}|^2 + |A_{CP}^{mix}|^2 + |A_{\Delta\Gamma}|^2 = 1$.

In eqns. (8,9) the crucial quantity λ_f is

$$\lambda_f = \left(\frac{q}{p} \right)_{B_s} \frac{A(\bar{B}_s \rightarrow f)}{A(B_s \rightarrow f)} \quad (10)$$

Neglecting terms of $O(\Gamma_{12}/M_{12})$ and assuming top dominance in the box diagram for the mixing, $(q/p)_{B_s}$ is a pure phase. Moreover, in the case of a CP eigenstate, if in the amplitude one has a dominant product of CKM matrix elements, $\frac{A(\bar{B}_s \rightarrow f_{CP})}{A(B_s \rightarrow f_{CP})}$ is also a pure phase. Under these conditions, $\lambda_{f_{CP}}$ is a pure phase.

Note however that if two different weak factors, affected by two different strong phases, contribute to the decay amplitude, the ratio $\frac{A(\bar{B}_s \rightarrow f_{CP})}{A(B_s \rightarrow f_{CP})}$ and a fortiori $\lambda_{f_{CP}}$, are not pure phases. This is the case within the QCDF framework since in the amplitude $A(\bar{B}_s \rightarrow f_{CP})$ the u and c quarks in the Penguin acquire different NLO QCD corrections.

In the case of two vector mesons like $\phi\phi$ the interference between mixing and decay now depends on the polarization,

$$\lambda_{\phi\phi}^{(k)} = \left(\frac{q}{p} \right)_{B_s} \frac{A(\bar{B}_s \rightarrow \phi\phi, k)}{A(B_s \rightarrow \phi\phi, k)} = \eta_k |\lambda_{\phi\phi}^{(k)}| e^{-i\phi_{\phi\phi}^{(k)}} \quad (11)$$

where k labels the polarization, longitudinal $k = L$, transverse parallel $k = \parallel$ and transverse perpendicular $k = \perp$, and η_k is the corresponding CP eigenvalue, $\eta_L = \eta_{\parallel} = +1$ and $\eta_{\perp} = -1$.

3.1 LHCb polarization-independent fit

LHCb finds, in a polarization-independent fit [1],

$$\lambda_{\phi\phi}^{(k)} = \eta_k |\lambda_{\phi\phi}| e^{-i\phi_s^{s\bar{s}s}} \quad (12)$$

$$\phi_s^{s\bar{s}s} = -0.073 \pm 0.115, \quad |\lambda_{\phi\phi}| = 0.99 \pm 0.05 \quad (13)$$

Although the quantity (12) is polarization-dependent because of the signs η_k , in the so-called "polarization-independent fit" of LHCb, the modulus $|\lambda_{\phi\phi}|$ and the phase $\phi_s^{s\bar{s}s}$ are assumed to be independent of the polarization. In Appendix B we compute in the QCDF scheme the quantities defined by (11), the moduli $|\lambda_{\phi\phi}^{(k)}|$ and the phases $\phi_{\phi\phi}^{(k)}$ for $k = L, \parallel, \perp$ and check that the hypothesis of a "polarization-independent fit" makes sense in a qualitative way.

To compare the theory with the LHCb data (13) we write now (11) with the notation

$$\lambda_{\phi\phi}^{(k)} = \eta_k \lambda_{\phi\phi} \quad (14)$$

$$\lambda_{\phi\phi} = |\lambda_{\phi\phi}| e^{-i\phi_{\phi\phi}} \quad (15)$$

Neglecting $\Delta\Gamma$ one finds the CP asymmetry,

$$\begin{aligned} A_{CP}^{mix}(t) &= \frac{\Gamma(\bar{B}_s(t) \rightarrow \phi\phi) - \Gamma(B_s(t) \rightarrow \phi\phi)}{\Gamma(\bar{B}_s(t) \rightarrow \phi\phi) + \Gamma(B_s(t) \rightarrow \phi\phi)} \\ &\simeq (f_L + f_{\parallel} - f_{\perp}) \text{Im}(\lambda_{\phi\phi}) \sin(\Delta Mt) = (1 - 2f_{\perp}) \text{Im}(\lambda_{\phi\phi}) \sin(\Delta Mt) \end{aligned} \quad (16)$$

On the other hand, if we assume the limit (5), $\bar{A}_+ = 0$, the CP asymmetry $A_{CP}^{mix}(t)$ can be expressed in terms of just the longitudinal polarization fraction $1 - 2f_{\perp} \simeq f_L$.

In conclusion, concerning the mixing CP asymmetry A_{CP}^{mix} in the case $\bar{B}_s \rightarrow \phi\phi$, assuming that the CP phase is the same for the different polarizations, as done in [1], one needs only f_{\perp} , or to a rather good approximation f_L , both already measured at LHCb, as shown in Table 1.

3.2 A_{CP}^{mix} for $\overline{B}_s \rightarrow \phi\phi$ with top dominance in mixing and Naive Factorization in decay

With top dominance one gets for the mixing,

$$\left(\frac{q}{p}\right)_{B_s} \simeq -\frac{M_{12}^*}{|M_{12}|} = -\sqrt{\frac{M_{12}^*}{M_{12}}} \simeq -\sqrt{\frac{(V_{tb}^*V_{ts})^2}{(V_{tb}V_{ts}^*)^2}} = -\frac{V_{tb}^*V_{ts}}{V_{tb}V_{ts}^*} \quad (17)$$

In the decay $B_s \rightarrow \phi\phi$ within NF the Penguin amplitude is proportional to $-V_{ts}^*V_{tb}$ with the coefficient $C_4 + C_3/N_c$, where the Wilson coefficients C_i are given in Table 11. Then we have, with the convention $CP | B \rangle = - | \overline{B} \rangle$,

$$\lambda_{\phi\phi} = \left(\frac{q}{p}\right)_{B_s} \frac{A(\overline{B}_s \rightarrow \phi\phi)}{A(B_s \rightarrow \phi\phi)} \simeq \left(-\frac{V_{tb}^*V_{ts}}{V_{tb}V_{ts}^*}\right) \left(-\frac{V_{ts}^*V_{tb}}{V_{ts}V_{tb}^*}\right) = 1 \quad (18)$$

and there is no CP violation in this limit.

4 Corrections to the cancellation of the CP phase

4.1 Corrections to mixing in the Standard Model

We consider here possible small corrections to the cancellation of CP violation in the SM (18) and in Section 5.1 we will introduce possible physics beyond the SM in mixing.

4.1.1 Contributions of other quarks to the box diagram

Unlike $K - \overline{K}$ mixing, that has large corrections from ct, cc corrections to tt in the box diagram loop, $B - \overline{B}$ mixing is dominated by the top. However, since in this latter case we are interested in the approximate cancellation between mixing and decay, let us compute the corrections to top dominance in mixing. Including (t, c, u) and using unitarity $V_{ub}V_{ud}^* = -V_{cb}V_{cd}^* - V_{tb}V_{td}^*$, one obtains [10],

$$\left(\frac{q}{p}\right)_{B_q} \simeq -\sqrt{\frac{(V_{tb}^*V_{tq})^2 S(x_t) + 2(V_{tb}^*V_{tq})(V_{cb}^*V_{cq})S(x_c, x_t) + (V_{cb}^*V_{cq})^2 S(x_c)}{(V_{tb}V_{tq}^*)^2 S(x_t) + 2(V_{tb}V_{tq}^*)(V_{cb}V_{cq}^*)S(x_c, x_t) + (V_{cb}V_{cq}^*)^2 S(x_c)}}} \quad (19)$$

From

$$x_i = \frac{m_i^2}{M_W^2}, \quad x_t \simeq 4.6, \quad x_c \simeq 3.5 \times 10^{-4} \quad (20)$$

one gets [11]

$$\begin{aligned}
S(x_t) &= x_t \left[\frac{1}{4} + \frac{9}{4} \frac{1}{(1-x_t)} - \frac{3}{2} \frac{1}{(1-x_t)^2} \right] - \frac{3}{2} \left(\frac{x_t}{1-x_t} \right)^3 \log x_t \simeq 2.5 \\
S(x_c) &\simeq x_c \simeq 3.5 \times 10^{-4} \\
S(x_c, x_t) &= x_c \left[\log \frac{x_t}{x_c} - \frac{3x_t}{4(1-x_t)} - \frac{3x_t^2 \log x_t}{4(1-x_t)^2} \right] \simeq 3 \times 10^{-3}
\end{aligned} \tag{21}$$

Finally one finds, taking into account both (c, t) in the mixing,

$$\left(\frac{q}{p} \right)_{B_s} = -0.9994 - 0.0350i \tag{22}$$

and, keeping only top dominance, one gets a very close result,

$$\left(\frac{q}{p} \right)_{B_s} = -0.9994 - 0.0349i \tag{23}$$

Therefore, the correction to top dominance is only of $O(10^{-4})$, and we can very safely make the approximation

$$\left(\frac{q}{p} \right)_{B_s} \simeq -\frac{V_{tb}^* V_{ts}}{V_{tb} V_{ts}^*} \tag{24}$$

4.1.2 Corrections to mixing of $O(\Gamma_{12}/M_{12})$

With the phase of M_{12} in the limit of top dominance being

$$\phi_M = \arg M_{12} = \arg (V_{tb} V_{ts}^*)^2 \tag{25}$$

the mixing parameter is given by [9],

$$\left(\frac{q}{p} \right)_{B_s} = -e^{-i\phi_M} \left(1 - \frac{a}{2} \right) \tag{26}$$

where the parameter a is given by

$$a = \frac{|\Gamma_{12}|}{|M_{12}|} \sin \phi \tag{27}$$

and the phase ϕ is defined by

$$\frac{M_{12}}{\Gamma_{12}} = -\frac{|M_{12}|}{|\Gamma_{12}|} e^{i\phi} \tag{28}$$

From

$$\Delta M = 2 | M_{12} | , \quad \Delta \Gamma = 2 | \Gamma_{12} | \quad (29)$$

we have therefore the upper bound

$$| a | \leq \frac{\Delta \Gamma}{\Delta M} \simeq \frac{0.091}{17.761} \simeq 5 \times 10^{-3} \quad (30)$$

From this bound we conclude that the correction to $\left(\frac{q}{p}\right)_{B_s}$ being the pure phase dominated by top exchange,

$$\left(\frac{q}{p}\right)_{B_s} = -e^{-i\phi_M} \quad (31)$$

is at most of $O(2.5 \times 10^{-3})$.

4.2 QCD Factorization corrections to the ratio of decay amplitudes $A(\bar{B}_s \rightarrow \phi\phi)/A(B_s \rightarrow \phi\phi)$

To go beyond the Naive Factorization calculation, the natural theoretical scheme is QCD Factorization (QCDF), that starts from short distance operators with their Wilson coefficients, including the Penguin and EW Penguin operators, given in Appendix A. Next, this scheme includes NLO $O(\alpha_s)$ Vertex corrections V , Penguin diagrams P , Hard Spectator diagrams H and Weak Annihilation A (Fig. 3).

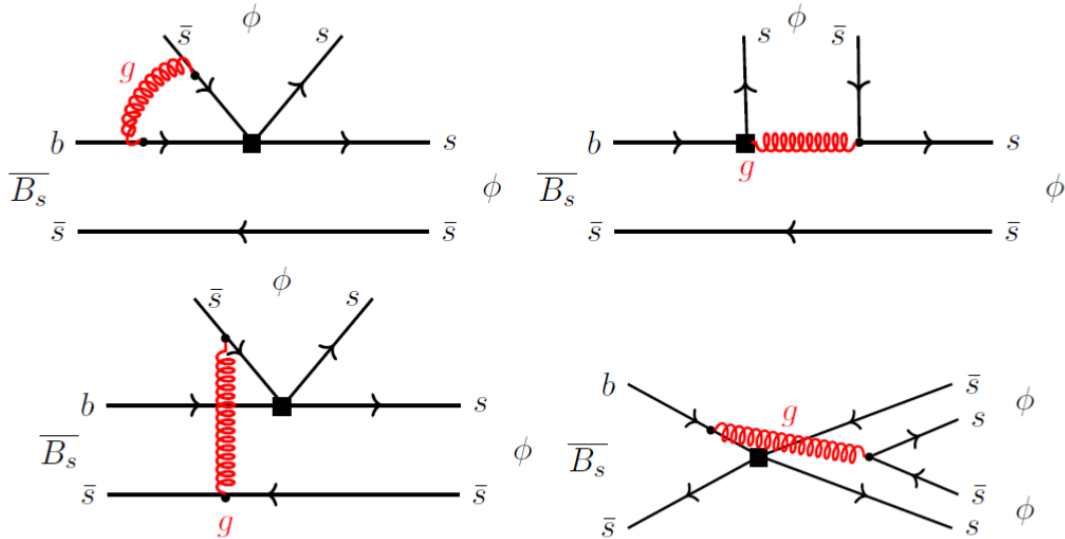


Fig. 3. Typical NLO α_s corrections of the QCDF scheme. From left to right and from above to below : corrections of the types Vertex V , Penguin P , Hard Spectator H and Annihilation A .

The Wilson coefficients C_i ($i = 1, \dots, 10$) at NLO [12], for $\mu = m_b$, with $m_b(m_b) = 4.2$ GeV, $\Lambda_{\overline{MS}}^{(5)} = 0.225$ GeV, are given in Table 11 of Appendix A.

Schematically, the matrix elements have the structure [13, 14, 15],

$$\begin{aligned} \langle V_1 V_2 | O_i | \overline{B} \rangle = & \left[F^{\overline{B} \rightarrow V_1} T_i^I \otimes f_{V_2} \Phi_{V_2} + (V_1 \leftrightarrow V_2) \right] \\ & + T_i^{II} \otimes f_B \Phi_B \otimes f_{V_1} \Phi_{V_1} \otimes f_{V_2} \Phi_{V_2} \end{aligned} \quad (32)$$

The first term depends on the form factor $F^{\overline{B} \rightarrow V_1}$ and decay constant f_{V_2} , the second is the Annihilation, dependent on the three decay constants f_B, f_{V_1}, f_{V_2} .

We would like to compare the theoretical prediction for A_{CP}^{mix} for $B_s \rightarrow \phi\phi$ with the LHCb measurement. Although other fits at LHCb have been tried that depend on the polarization, the data (12,13) have been obtained assuming the CP-violating phases to be independent of the polarization. To this aim, we will concentrate now on just one polarization, namely the longitudinal one $h = 0$, studied in great detail in [5].

The longitudinal decay amplitude for $B_s \rightarrow \phi\phi$ reads, with a sum over the quarks $p = u, c$,

$$A(\overline{B}_s \rightarrow \phi\phi, h = 0) = \sum_{p=u,c} \lambda'_p S^{p,0} A_{\phi\phi}^0 + (\lambda'_u + \lambda'_c) T^0 B_{\phi\phi}^0 \quad (33)$$

and to get the amplitude $A(B_s \rightarrow \phi\phi, h = 0)$ one needs to replace in (33) $\lambda'_p \rightarrow \lambda'_p^*$ ($p = u, c$).

For the sake of simplicity, we begin to analyze first the trend of the different observables within the QCDF scheme by using central values of the different parameters. We will later, in sections 5, 6.4 and 7.6, take into account the relevant errors.

The amplitude (33) depends on the quantities listed here below :

- the CKM factors

$$\lambda'_p = V_{pb} V_{ps}^* \quad (p = u, c) , \quad (34)$$

given by

$$\lambda'_u = V_{ub} V_{us}^* = 0.00030 - 0.00076 i , \quad \lambda'_c = V_{cb} V_{cs}^* = 0.039 , \quad (35)$$

- the coefficients $A_{\phi\phi}^0, B_{\phi\phi}^0$ in (33), that correspond respectively to the direct diagram and to the annihilation diagram, given by

$$A_{\phi\phi}^0 = i \frac{G_F}{\sqrt{2}} m_{B_s}^2 A_0^{B_s \rightarrow \phi}(m_\phi^2) f_\phi , \quad m_{B_s}^2 A_0^{B_s \rightarrow \phi}(m_\phi^2) f_\phi = 3.00 \text{ GeV}^3 \quad (36)$$

$$B_{\phi\phi}^0 = i \frac{G_F}{\sqrt{2}} f_{B_s} f_\phi f_\phi, \quad f_{B_s} f_\phi f_\phi = 1.12 \times 10^{-2} \text{ GeV}^3 \quad (37)$$

for the form factor and decay constants of [5]

- the combinations of coefficients

$$\begin{aligned} S^{p,0} &= 2 \left(a_4^{p,0} + a_3^0 + a_5^0 - \frac{1}{2} (a_7^{p,0} + a_9^{p,0} + a_{10}^{p,0}) \right) \\ T^0 &= 2 \left(b_3^0 + b_4^0 - \frac{1}{2} (b_3^{EW,0} + b_4^{EW,0}) \right) \end{aligned} \quad (38)$$

The coefficients a_i^0, b_i^0 in (38) are given by the short distance Wilson coefficients with the inclusion of the $O(\alpha_s)$ corrections of QCDF that depend now on the longitudinal polarization.

In QCD Factorization, the coefficients a_i^h depend on the helicity. To fix the ideas, we write down their general expression given in the Appendix of [3],

$$a_i^{p,h}(V_1 V_2) = \left(C_i + \frac{C_{i\pm 1}}{N_c} \right) N_i^h(V_2) + \frac{C_{i\pm 1}}{N_c} \frac{C_F \alpha_s}{4\pi} \left[V_i^h(V_2) + \frac{4\pi^2}{N_c} H_i^h(V_1 V_2) \right] + P_i^{p,h}(V_2) \quad (39)$$

where C_i are the short distance Wilson coefficients tabulated in Appendix A, the upper (lower) signs correspond to i odd (even), N_i are normalization factors, V_i are the vertex corrections, H_i are the hard scattering corrections, and P_i are the Penguin corrections. The Annihilation corrections b_i^h are not included in this formula.

In the limit of disregarding the NLO α_s corrections, the coefficients (39) become the usual combinations of short distance Wilson coefficients, e.g. $a_4^{p,h} \rightarrow C_4 + \frac{C_3}{N_c}, \dots$ where the C_i are given in Appendix A, while the annihilation coefficients $b_i^h \rightarrow 0$.

The coefficients at NLO are given in Table 2.

$a_3^0 + a_5^0$		$a_4^{u,0}$	$a_4^{c,0}$
0.002 - 0.001 <i>i</i>		-0.025 - 0.016 <i>i</i>	-0.033 - 0.009 <i>i</i>
$(a_7^{u,0} + a_9^{u,0})/\alpha$	$(a_7^{c,0} + a_9^{c,0})/\alpha$	$a_{10}^{u,0}/\alpha$	$a_{10}^{c,0}/\alpha$
-1.84 - 0.54 <i>i</i>	-1.10 - 0.02 <i>i</i>	-0.17 + 0.09 <i>i</i>	-0.17 + 0.09 <i>i</i>

Table 2. Coefficients at NLO used in QCD Factorization for helicity $h = 0$ [5].

For Annihilation diagrams one has the parameters of Table 3.

Model	$r_A b_3^0$	$r_A b_4^0$	$r_A b_3^{EW,0}/\alpha$	$r_A b_4^{EW,0}/\alpha$
(1)	0.003	-0.003	-0.035	0.013
(2)	0.017 - 0.018 i	-0.006 + 0.002 i	-0.080 + 0.051 i	0.023 - 0.009 i

Table 3. Coefficients for $h = 0$ annihilation, with $r_A = B_{\rho\rho}/A_{\rho\rho} = 5. \times 10^{-3}$, from $f_{B_d} = 0.200$ GeV, $f_\rho = 0.209$ GeV, $A_0^{B_d \rightarrow \rho}(0) = 0.30$ and $\alpha = 1/129$ [5]. Model (1) uses the default value $X_A = \ln \frac{m_B}{\Lambda_h}$ for the power-suppressed annihilation contributions [5], and the results for model (2) are obtained in Appendix C, with $X_A = \left(1 + \rho_A e^{i\phi_A}\right) \ln \frac{m_B}{\Lambda_h}$ and $\rho_A = 0.6, \phi_A = -40^\circ$ from [3].

From the parameters of Tables 2 and 3 we find the factors relevant to eq. (33),

$$\begin{aligned}
S^{u,0} &= a_4^{u,0} + a_3^0 + a_5^0 - \frac{1}{2}(a_7^{u,0} + a_9^{u,0} + a_{10}^{u,0}) = -0.0304 - 0.0306i \\
S^{c,0} &= a_4^{c,0} + a_3^0 + a_5^0 - \frac{1}{2}(a_7^{c,0} + a_9^{c,0} + a_{10}^{c,0}) = -0.0522 - 0.0205i \\
T^0 &= b_3^0 + b_4^0 - \frac{1}{2}(b_3^{EW,0} + b_4^{EW,0}) = 0.0342
\end{aligned} \tag{40}$$

We have, with a sum over $p = u, c$, the ratio

$$\left(\frac{A(\overline{B}_s \rightarrow \phi\phi, h=0)}{A(B_s \rightarrow \phi\phi, h=0)} \right)_{QCDF} = - \frac{\sum_{p=u,c} \lambda'_p S^{p,0} A_{\phi\phi}^0 + (\lambda'_u + \lambda'_c) T^0 B_{\phi\phi}^0}{\sum_{p=u,c} (\lambda'_p)^* S^{p,0} A_{\phi\phi}^0 + [(\lambda'_u)^* + (\lambda'_c)^*] T^0 B_{\phi\phi}^0} \tag{41}$$

Using the central values given by Tables 2 and 3 (Model (1)), and (36,37) we get

$$\left(\frac{A(\overline{B}_s \rightarrow \phi\phi, h=0)}{A(B_s \rightarrow \phi\phi, h=0)} \right)_{QCDF} = -1.003 + 0.031i \tag{42}$$

Therefore, the departure from the NF value $-\frac{V_{tb}V_{ts}^*}{V_{tb}^*V_{ts}} = -0.999 + 0.035i$ is of the order of the percent.

4.3 Time-dependent CP violation in QCD Factorization

We will now use the notation of Bartsch et al. [5], and their formulas (74) and (113),

$$a_p = S^{p,0} m_{B_s}^2 A_0^{B_s \rightarrow \phi}(m_\phi^2) f_\phi + T^0 f_{B_s} f_\phi f_\phi \tag{43}$$

where $a_p(p = u, c)$ are the coefficients of $i\frac{G_F}{\sqrt{2}}\lambda'_p$ ($p = u, c$) of the total $\overline{B}_s \rightarrow \phi_L\phi_L$ amplitude (33), with the CKM factors λ'_p ($p = u, c$) defined by (34).

Let us write the Standard Model quantity

$$\lambda_{\phi\phi}^{SM} = \left(\frac{q}{p}\right)_{B_s} \left(\frac{A(\overline{B}_s \rightarrow \phi\phi, h=0)}{A(B_s \rightarrow \phi\phi, h=0)}\right)_{QCDF} \quad (44)$$

with the mixing computed from the box diagram

$$\left(\frac{q}{p}\right)_{B_s} \simeq -\frac{V_{tb}^* V_{ts}}{V_{tb} V_{ts}^*} \simeq -\frac{V_{ub}^* V_{us} + V_{cb}^* V_{cs}}{V_{ub} V_{us}^* + V_{cb} V_{cs}^*} = -\frac{\lambda_u'^* + \lambda_c'^*}{\lambda_u' + \lambda_c'} \quad (45)$$

and the decay amplitude estimated using QCDF,

$$\left(\frac{A(\overline{B}_s \rightarrow \phi\phi, h=0)}{A(B_s \rightarrow \phi\phi, h=0)}\right)_{QCDF} = -\frac{\lambda_c' a_c + \lambda_u' a_u}{\lambda_c'^* a_c + \lambda_u'^* a_u} = -\frac{a_c + \lambda^2(\rho - i\eta)a_u}{a_c + \lambda^2(\rho + i\eta)a_u} \quad (46)$$

where $\lambda = 0.226$, $\rho = 0.141$ and $\eta = 0.357$ are CKM parameters.

The time-dependent CP asymmetry writes, in the limit of neglecting the width difference $\Delta\Gamma_s$,

$$A_\phi^{CP}(t) = S_\phi \sin(\Delta M_s t) - C_\phi \cos(\Delta M_s t) \quad (47)$$

$$S_\phi = \frac{2\text{Im}\lambda_{\phi\phi}}{1 + |\lambda_{\phi\phi}|^2}, \quad C_\phi = \frac{1 - |\lambda_{\phi\phi}|^2}{1 + |\lambda_{\phi\phi}|^2}, \quad \lambda_{\phi\phi} = -\frac{M_{12}^*}{|M_{12}|} \frac{A(\overline{B}_s \rightarrow \phi\phi, h=0)}{A(B_s \rightarrow \phi\phi, h=0)} \quad (48)$$

Particularizing to the longitudinal polarization $\phi_L\phi_L$ and QCDF, and expanding in powers of the Wolfenstein parameter λ one finds,

$$\begin{aligned} \lambda_{\phi\phi}^L &= \left(\frac{q}{p}\right)_{B_s} \left(\frac{A(\overline{B}_s \rightarrow \phi\phi, h=0)}{A(B_s \rightarrow \phi\phi, h=0)}\right)_{QCDF} = \frac{\lambda_u'^* + \lambda_c'^*}{\lambda_u' + \lambda_c'} \frac{\lambda_c' a_c + \lambda_u' a_u}{\lambda_c'^* a_c + \lambda_u'^* a_u} \\ &\simeq 1 + 2\lambda^2\eta \left[-\text{Im}\left(\frac{a_c - a_u}{a_c}\right) + i \text{Re}\left(\frac{a_c - a_u}{a_c}\right) \right] \end{aligned} \quad (49)$$

In the limit of NF one has $a_c = a_u$ and therefore $\lambda_{\phi\phi}^{NF} = 1$.

One gets, with the definition (15),

$$|\lambda_{\phi\phi}^L| \simeq 1 - 2\lambda^2\eta \text{Im}\left(\frac{a_c - a_u}{a_c}\right) \quad (50)$$

$$\phi_{\phi\phi}^L \simeq -2\lambda^2\eta \text{Re}\left(\frac{a_c - a_u}{a_c}\right) \quad (51)$$

From the values of the coefficients given in Tables 2 and 3 for Model (1) and the form factor $A_{\phi\phi}^0 = 0.47$ [5], one gets

$$\begin{aligned} a_c &= -0.156 - 0.062i, \quad a_u = -0.091 - 0.091i, \quad \frac{a_c - a_u}{a_c} = 0.296 - 0.308i \\ |a_c| &= 0.168 \text{ GeV}^3, \quad |a_c - a_u| = 0.072 \text{ GeV}^3 \end{aligned} \quad (52)$$

and therefore

$$|\lambda_{\phi\phi}^L| \simeq 1.011, \quad \phi_{\phi\phi}^L \simeq -0.011 \quad (53)$$

hence,

$$S_{\phi_L} = 2\lambda^2\eta \operatorname{Re}\left(\frac{a_c - a_u}{a_c}\right) = 0.011, \quad C_{\phi_L} = 2\lambda^2\eta \operatorname{Im}\left(\frac{a_c - a_u}{a_c}\right) = -0.011 \quad (54)$$

On the other hand, from the values of the coefficients given in Tables 2 and 3 for Model (2) and the form factor $A_{\phi\phi}^0 = 0.38$ [3], that we will adopt below, one gets

$$a_c = -0.076 - 0.122i, \quad a_u = -0.023 - 0.147i \quad (55)$$

and therefore

$$|\lambda_{\phi\phi}^L| \simeq 1.015, \quad \phi_{\phi\phi}^L \simeq 10^{-3} \quad (56)$$

4.4 Bounds on the modulus and phase of $\lambda_{\phi\phi}^L$

Going beyond the central values of Tables 2 and 3, that lead to (53), following Bartsch et al. [5] one can bound the modulus and phase of $\lambda_{\phi\phi}^L$.

Bartsch et al. have computed $|a_c - a_u|$ in QCD Factorization, finding

$$|a_c - a_u| \simeq 0.057 \text{ GeV}^3 \quad (57)$$

On the other hand, since $|\lambda'_u| \ll |\lambda'_c|$, one can compute $|a_c|$ from the longitudinal branching ratio $B(\overline{B}_s \rightarrow \phi\phi, h=0)$,

$$|a_c| = 0.177 \text{ GeV}^3 \left[\frac{B(\overline{B}_s \rightarrow \phi\phi, h=0)}{18.7 \times 10^{-6}} \right]^{1/2} \left[\frac{1.515 \text{ ps}}{\tau_{B_s}} \right]^{1/2} \quad (58)$$

At LHCb [1] the longitudinal fraction has been measured, as shown in Table 1, yielding,

$$B(\overline{B}_s \rightarrow \phi\phi, h=0) \simeq 0.38 \times B(\overline{B}_s \rightarrow \phi\phi) \simeq 7.1 \times 10^{-6} \quad (59)$$

and therefore,

$$|a_c| \simeq 0.11 \quad (60)$$

On the other hand, using (57,60), one has the upper bounds [5],

$$2\lambda^2\eta \operatorname{Re}\left(\frac{a_c - a_u}{a_c}\right) \leq 2\lambda^2\eta \frac{|a_c - a_u|}{|a_c|} \simeq 0.019$$

$$2\lambda^2\eta \operatorname{Im}\left(\frac{a_c - a_u}{a_c}\right) \leq 2\lambda^2\eta \frac{|a_c - a_u|}{|a_c|} \simeq 0.019 \quad (61)$$

and therefore,

$$|\lambda_{\phi\phi}^L| \geq 0.981 \quad (62)$$

$$\phi_{\phi\phi}^L \geq -0.019 \quad (63)$$

These bounds are not very constraining, and lie within the range of LHCb (13).

Following Bartsch et al. [5] one finds the upper bound,

$$S_\phi \leq 2\lambda^2\eta \frac{|a_c - a_u|}{|a_c|} \simeq 0.019 \quad (64)$$

and similarly for the modulus $|C_\phi|$.

5 Comparison of LHCb data with the SM and QCD Factorization

To summarize Section 3.2, let us recall that we have found, with top dominance in mixing and NF in decay,

$$|\lambda_{\phi\phi}| = 1, \quad \phi_{\phi\phi} = 0 \quad (65)$$

The different effects that go beyond NF, given by QCDF (53), obtained from the central values of the QCDF coefficients of Tables 2 and 3, are consistent within errors with the LHCb polarization-independent fit (13).

One could conversely look for the range of the QCDF parameters that are allowed by the LHCb data.

From (49) we get the experimental constraint

$$1 + 2\lambda^2\eta \left[-\operatorname{Im}\left(\frac{a_c - a_u}{a_c}\right) + i \operatorname{Re}\left(\frac{a_c - a_u}{a_c}\right) \right] = \lambda_{\phi\phi}^{LHCb} \quad (66)$$

From the LHCb data for $\lambda_{\phi\phi}^{LHCb}$ and the SM value $\lambda_{\phi\phi}^{SM}$, we realize that they are rather close and we can expand the precedent relation in the small quantities

$$\lambda^2, \quad |\lambda_{\phi\phi}^{LHCb}| - 1, \quad \phi_{\phi\phi}^{LHCb} \quad (67)$$

giving the two relations

$$|\lambda_{\phi\phi}^{LHCb}| - 1 = -2\lambda^2\eta \operatorname{Im}\left(\frac{a_c - a_u}{a_c}\right) \quad (68)$$

$$\phi_{\phi\phi}^{LHCb} = -2\lambda^2\eta \operatorname{Re}\left(\frac{a_c - a_u}{a_c}\right) \quad (69)$$

From the values of LHCb (13), one gets

$$2\lambda^2\eta \operatorname{Im}\left(\frac{a_c - a_u}{a_c}\right) = 0.01 \pm 0.05 \quad (70)$$

$$2\lambda^2\eta \operatorname{Re}\left(\frac{a_c - a_u}{a_c}\right) = 0.073 \pm 0.115 \quad (71)$$

to be compared with (54), obtained from the central values in Tables 2 and 3(1).

Interestingly, from the LHCb data, or in the future from other experiments, if one assumes the CKM matrix for the electroweak sector, one could measure the QCDF quantities $\operatorname{Re}\left(\frac{a_c - a_u}{a_c}\right)$ and $\operatorname{Im}\left(\frac{a_c - a_u}{a_c}\right)$.

5.1 Including New Physics in mixing

We now go beyond the SM, and compare theory and experiment including NP contributions. A usual parametrization of a NP contribution to mixing is the following (see ref. [16] and references therein),

$$M_{12}^s = M_{12}^{SM,s} \Delta_s = M_{12}^{SM,s} (\operatorname{Re} \Delta_s + i \operatorname{Im} \Delta_s) = M_{12}^{SM,s} |\Delta_s| e^{i\phi_s^\Delta} \quad (72)$$

$$\phi_s = \phi_s^{SM} + \phi_s^\Delta$$

where $M_{12}^{SM,s}$, ϕ_s^{SM} stand for Standard Model values and the complex parameter Δ_s for New Physics, the SM corresponding to $(\operatorname{Re}\Delta_s, \operatorname{Im}\Delta_s) = (1, 0)$. On the other hand, we observe that the LHCb measurement is rather close to the SM values, but we would like to know which domain in the plane $(\operatorname{Re}\Delta_s, \operatorname{Im}\Delta_s)$ is still allowed from the data.

Including NP contributions, as in (72), one has from LHCb the experimental constraint on the NP parameters,

$$\lambda_{\phi\phi}^{SM} \sqrt{\frac{\Delta_s^*}{\Delta_s}} = \lambda_{\phi\phi}^{LHCb} \quad (73)$$

where $\lambda_{\phi\phi}^{SM}$ is given by (49) and $\lambda_{\phi\phi}^{LHCb}$ by (12,13).

Let us now look for the constraint on the NP mixing parameters. From (72,73) and the expansion (49) we get

$$\left\{ 1 + 2\lambda^2\eta \left[-\operatorname{Im}\left(\frac{a_c - a_u}{a_c}\right) + i \operatorname{Re}\left(\frac{a_c - a_u}{a_c}\right) \right] \right\} \sqrt{\frac{\operatorname{Re}\Delta_s - i\operatorname{Im}\Delta_s}{\operatorname{Re}\Delta_s + i\operatorname{Im}\Delta_s}} = \lambda_{\phi\phi}^{LHCb} \quad (74)$$

or, up to small SM terms of $O(\lambda^4)$,

$$\left[1 - 2\lambda^2\eta \operatorname{Im}\left(\frac{a_c - a_u}{a_c}\right)\right] e^{-i\phi_{\phi\phi}^{SM}} e^{-i\phi_s^\Delta} = \lambda_{\phi\phi}^{LHCb} \quad (75)$$

with (51),

$$\phi_{\phi\phi}^{SM} = -2\lambda^2\eta \operatorname{Re}\left(\frac{a_c - a_u}{a_c}\right) \quad (76)$$

and, from (13), eqn. (75) implies the two constraints,

$$1 - 2\lambda^2\eta \operatorname{Im}\left(\frac{a_c - a_u}{a_c}\right) = |\lambda_{\phi\phi}^{LHCb}| = 0.99 \pm 0.05 \quad (77)$$

$$\phi_s^\Delta = -\phi_{\phi\phi}^{SM} + \phi_{\phi\phi}^{LHCb} = -\phi_{\phi\phi}^{SM} + (-0.073 \pm 0.115) \quad (78)$$

Notice that the first constraint (77) concerns only the SM quantity $2\lambda^2\eta \operatorname{Im}\left(\frac{a_c - a_u}{a_c}\right) = -0.011$ (54), while the second constraint (78) involves SM model and NP quantities.

The first constraint (77) writes 1.011 in the l.h.s. vs. the r.h.s. LHCb value 0.99 ± 0.05 , and it is satisfied within errors.

From the second constraint (78), and (53) $\phi_{\phi\phi}^{SM} \simeq -0.011$, one obtains for the NP parameter

$$\frac{\operatorname{Im}\Delta_s}{\operatorname{Re}\Delta_s} \simeq -0.062 \pm 0.115 \quad (79)$$

i.e.,

$$-0.177 \leq \frac{\operatorname{Im}\Delta_s}{\operatorname{Re}\Delta_s} \leq 0.053 \quad (80)$$

that gives the domain in Fig. 4, from the 1σ error of the LHCb CP phase.

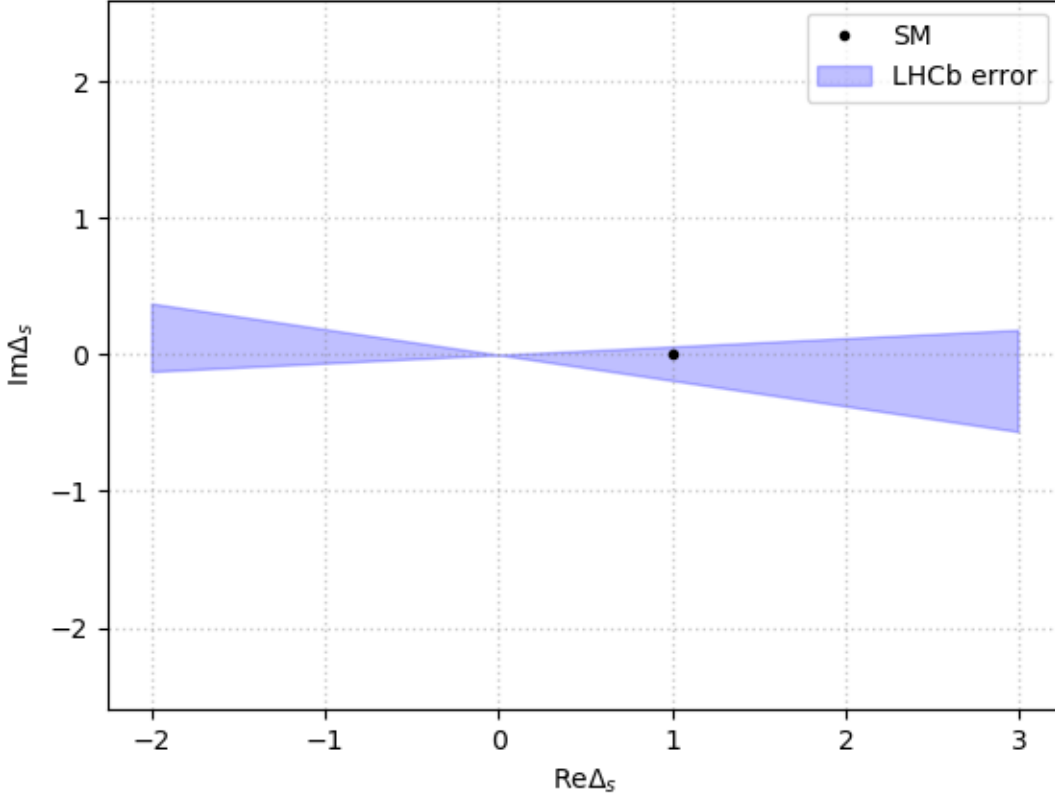


Fig. 4. Domain allowed in the plane $\text{Re}\Delta_s$ - $\text{Im}\Delta_s$ from $B_s \rightarrow \phi\phi$ LHCb data. If one takes into account the constraints from other observables, as exposed for example in ref. [16], then only the domain for $\text{Re}\Delta_s > 0$ remains.

This domain is comparable to the domain allowed by other observables, in particular from the decay $\bar{B}_s \rightarrow J/\psi\phi$, e.g. by CKMfitter [16].

We conclude that the mode $B_s \rightarrow \phi\phi$, combined with other observables, can be useful in the future to look for or to discard NP contributions.

6 Expected sensitivity at FCCee and implications in the search for NP

FCCee is a fantastic source of B mesons when operating at the Z-pole thanks to the relatively large cross section for the production of Z bosons (~ 42.9 nb) and the large

instantaneous luminosity of $2.3 \cdot 10^{36} \text{ cm}^{-2}\text{s}^{-1}$, which is planned for. Furthermore it is foreseen to operate the collider with at least 2 detectors for 4 years at the Z-pole so that a total integrated luminosity of 150 ab^{-1} can be accumulated. As a consequence, a large number of $\overline{B}_s(B_s) \rightarrow \phi\phi$ ($\sim 9.4 \cdot 10^5$) is expected as summarized in Table 4. In the following, we use a parametrized detector to evaluate the sensitivities, which can be achieved at FCCee [18, 19, 20].

$E_{\text{cm}} = 91.2 \text{ GeV}$ $\int L = 150\text{ab}^{-1}$			
$\sigma(e^+e^- \rightarrow Z)$	number	f[Z $\rightarrow \overline{B}_s(\overline{B}_d)$]	Number of
nb	of Z		produced $\overline{B}_s(\overline{B}_d)$
~ 42.9	$\sim 6.4 \cdot 10^{12}$	0.0159(0.0608)	$\sim 1 \cdot 10^{11}(3.9 \cdot 10^{11})$
$\overline{B}_{d,s}$ decay	ϕ decay	Final	Number of
Mode	Mode	State	$\overline{B}_{d,s}$ decays
$\overline{B}_d \rightarrow \phi\phi$	$\phi \rightarrow K^+K^-$	$K^+K^-K^+K^-$	$\sim 2.9 \cdot 10^2$
$\overline{B}_s \rightarrow \phi\phi$	$\phi \rightarrow K^+K^-$	$K^+K^-K^+K^-$	$\sim 4.7 \cdot 10^5$

Table 4. The expected numbers of produced $\overline{B}_s(\overline{B}_d)$ decays to the specific decay mode $\overline{B}_s(\overline{B}_d) \rightarrow \phi\phi$ at FCC-ee at a center of mass energy of 91.2 GeV over 4 years with 2 detectors. These numbers have to be multiplied by 2 when including $B_s(B_d)$ decays. The branching fractions of the PDG [17] have been used for $\overline{B}_s \rightarrow \phi\phi$, while it is estimated to $\sim 3 \cdot 10^{-9}$ using QCDF for $\overline{B}_d \rightarrow \phi\phi$.

6.1 Generic detector resolutions

In order to carry out experimental studies, we define a generic detector, the resolution of which is parametrized as follow :

$$\begin{array}{l}
 \text{Acceptance :} \quad |\cos \theta| < 0.95 \\
 \hline
 \text{Charged particles :} \\
 p_T \text{ resolution :} \quad \frac{\sigma(p_T)}{p_T^2} = 2. \times 10^{-5} \oplus \frac{1.2 \times 10^{-3}}{p_T \sin \theta} \\
 \phi, \theta \text{ resolution :} \quad \sigma(\phi, \theta) \mu\text{rad} = 18 \oplus \frac{1.5 \times 10^3}{p_T \sqrt[3]{\sin \theta}} \\
 \text{Vertex resolution :} \quad \sigma(d_{\text{Im}}) \mu\text{m} = 1.8 \oplus \frac{5.4 \times 10^1}{p_T \sqrt{\sin \theta}} \\
 \hline
 \text{e, } \gamma \text{ particles :} \\
 \text{Energy resolution :} \quad \frac{\sigma(E)}{E} = \frac{5 \times 10^{-2}}{\sqrt{E}} \oplus 5 \times 10^{-3} \\
 \text{EM } \phi, \theta \text{ resolution :} \quad \sigma(\phi, \theta) \text{ mrad} = \frac{7}{\sqrt{E}} \\
 \hline \hline
 \end{array} \tag{81}$$

where θ, ϕ are the particles' polar and azimuthal angles respectively, p_T (in GeV) the track transverse momentum, E the e^\pm, γ energy and d_{Im} the tracks' impact parameter.

With the detector resolutions in (81) and a reasonably good particle identification system (ToF + cluster counting for dE/dx), a clean signal for $\overline{B}_s(B_s) \rightarrow \phi\phi$ is expected. The main source of background is the combinatorial one, which is however expected to be small (Background/Signal < 10%), thanks to a good particle identification system and the excellent mass resolution for ϕ and B_s as shown in Figure 5 for the latter.

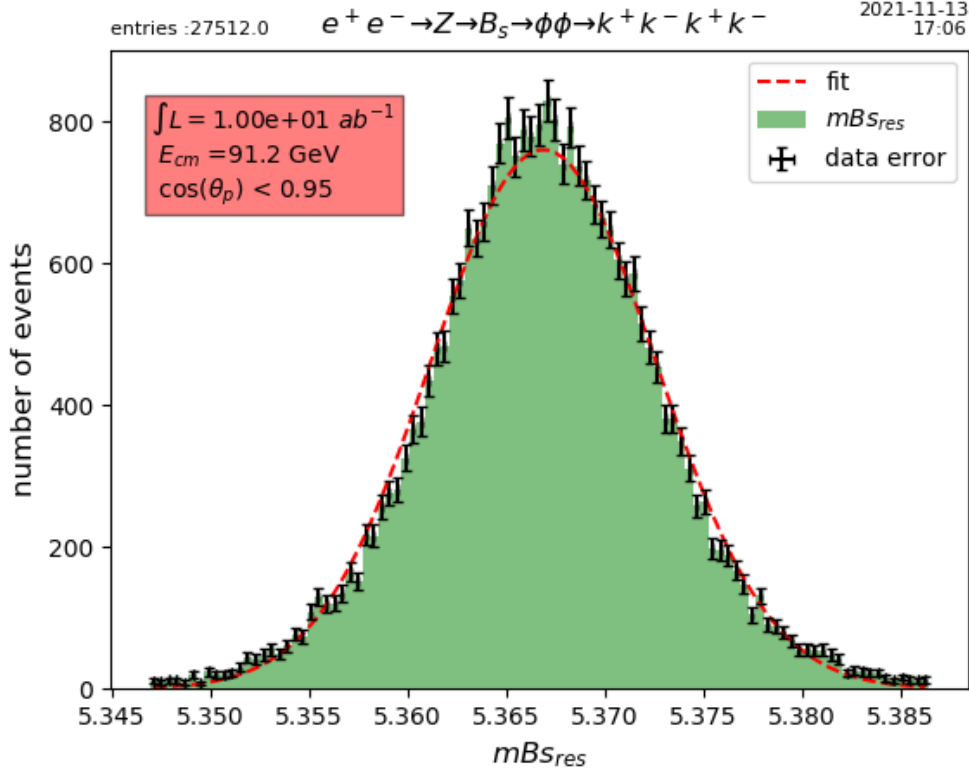


Fig. 5. B_s mass resolution for $\overline{B}_s(B_s) \rightarrow \phi\phi \rightarrow K^+K^-K^+K^-$ decay. One obtains $\sigma(m_{B_s}) \simeq 5.7$ MeV. The geometric acceptance of the detector ($|\cos\theta| < .95$) leads to an efficiency of 86% for this 4-body final state. The combinatorial background is not shown in this figure.

6.2 Experimental expectations for CP violation parameters at FCCee

We use eq. (8) to obtain the decay widths for $\overline{B}_s(B_s) \rightarrow \phi\phi$ and we include the wrong tagging fraction ω ,

$$\begin{aligned}
\Gamma(\overline{B}_s \rightarrow \phi\phi) &= |\langle \phi\phi | B_s \rangle|^2 \times e^{-\Gamma t} \left\{ \cosh \frac{\Delta\Gamma}{2} - (1 - 2\omega) A_{CP}^{dir} \cos \Delta mt \right. \\
&\quad \left. + A_{\Delta\Gamma} \sinh \frac{\Delta\Gamma}{2} - (1 - 2\omega) A_{CP}^{mix} \sin \Delta mt \right\} \\
\Gamma(B_s \rightarrow \phi\phi) &= |\langle \phi\phi | B_s \rangle|^2 \times e^{-\Gamma t} \left\{ \cosh \frac{\Delta\Gamma}{2} + (1 - 2\omega) A_{CP}^{dir} \cos \Delta mt \right. \\
&\quad \left. + A_{\Delta\Gamma} \sinh \frac{\Delta\Gamma}{2} + (1 - 2\omega) A_{CP}^{mix} \sin \Delta mt \right\}
\end{aligned} \tag{82}$$

It is important to note that the $\Delta\Gamma$ -dependent terms enable one to solve the ambiguity for the determination of the CP violating phase $\phi_{\phi\phi}$. We have verified that keeping $\Delta\Gamma$ as a free parameter in the fit does not degrade significantly the sensitivity obtained in this study for the parameters $|\lambda_{\phi\phi}|$ and the CP violating phase $\phi_{\phi\phi}$. However the determination of $\Delta\Gamma$ is not the main topic in this study as it can be obtained with higher precision by studying other modes such as $B_s \rightarrow J/\psi \phi$ and $B_s \rightarrow J/\psi \eta$.

As shown in equation (16), A_{CP}^{mix} depends on η_f , the CP eigenvalue of the final state. For a V_1 - V_2 final state such as $\phi\phi$, η_f varies as a function of the polarization state. For $\phi\phi$, it is $\eta_f = +1$ for the longitudinal and parallel polarizations while $\eta_f = -1$ for the perpendicular polarization. In case one does not disentangle the polarization by doing a full angular analysis, one would have an effective $\eta_{\phi\phi}^{eff} = 1 - 2f_{\perp} = 0.416 \pm 0.018$ as obtained from the experimentally measured polarizations [?] summarized in Table 1. Since it is expected in the Standard Model that $|\lambda_{\phi\phi}| \simeq 1$, we simplify $A_{CP}^{mix} \simeq -\eta_{\phi\phi}^{eff} \sin \phi_{\phi\phi}$, where $\phi_{\phi\phi}$ is the phase responsible of CP violation.

As one can see in equation (82), CP violating effects are damped by the fraction of wrong tagging, ω (Table 5 shows typical tagging performances of some experiments).

Tagging Merit	LEP	BaBar	LHCb
$\epsilon(1 - 2\omega)^2$	25-30%	30%	6%

Table 5. Typical tagging Figure of Merit for some experiments. ϵ is the tagging efficiency and ω , the wrong tagging fraction, which is in the range $0 - 0.5$.

It is thus essential to measure this factor precisely. Fortunately, the large statistics at FCCee enables one to measure the value of ω very precisely, for example with the decay $\overline{B}_s \rightarrow D_s^+ \pi^- \rightarrow \phi \pi^+ \pi^-$, which is similar to the final state $\phi\phi$ (see [21] for details). With this very clean and abundant mode, ω can be determined with a negligible error. In the following, we assume $\omega = 0.25$, which is rather conservative since it was achieved at LEP.

Another important factor to consider is the detector resolution for the reconstruction of the B_s vertex. A detailed simulation study has been done in a previous

paper for the mode $B_s \rightarrow J/\psi\phi$ [21], which is a final state rather similar to $\phi\phi$. We have found that a resolution of $\sim 20 \mu\text{m}$ can be obtained, which does not affect significantly the resolution on $\phi_{\phi\phi}$ (i.e. 2 – 3% level), and can thus be safely corrected for. Indeed, this vertex resolution of $20 \mu\text{m}$ has to be compared to the average B_s flight distance of about 3mm at the Z-pole.

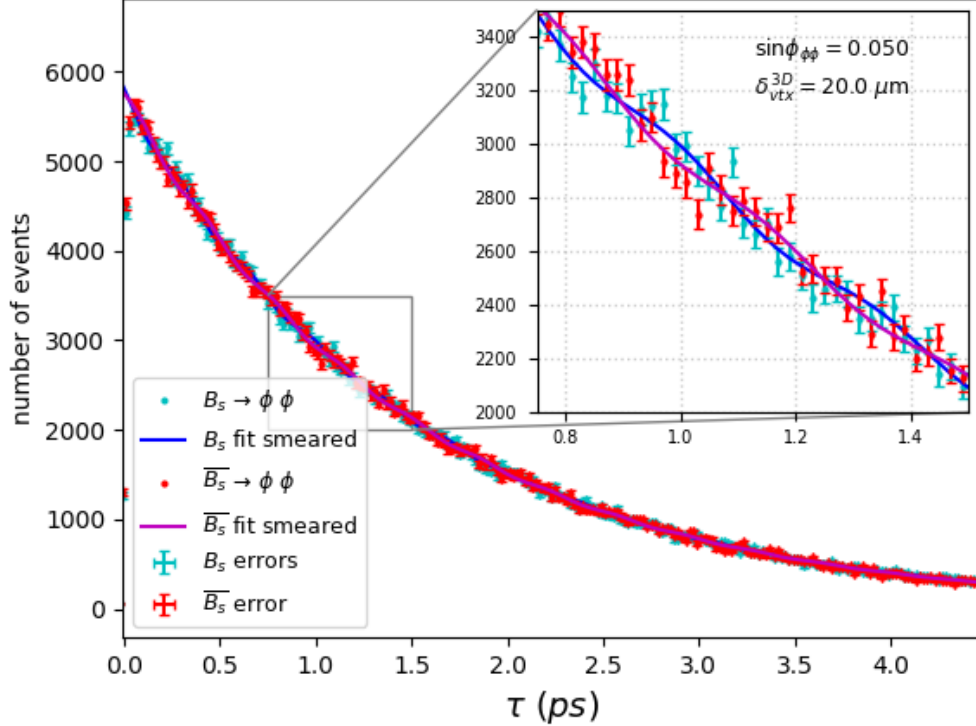


Fig. 6. The time-dependent distributions for the simulated $\overline{B}_s(B_s) \rightarrow \phi\phi$ events are shown with the statistics of 150 ab^{-1} expected at FCCee. The input parameters $|\lambda_{\phi\phi}| = 1$, $\phi_{\phi\phi} = 0.05$, $\eta_{\phi\phi} = 0.416$, $\Delta\Gamma = 0$, and $\omega = 0.25$ have been used.

To estimate the sensitivity, which can be achieved at FCCee, we assume the input parameters $|\lambda_{\phi\phi}| = 1$, $\phi_{\phi\phi} = 0.05$ and $\eta_{\phi\phi}^{eff} = 0.416$, and generate the time-dependent signal events accordingly. Figure 6 shows a typical time-dependent spectrum of the signal, which is expected in an experiment with the integrated statistics of 150 ab^{-1} .

We then repeat such experiment 5000 times and extract the distributions for the fitted variables $|\lambda_{\phi\phi}|$ and $\phi_{\phi\phi}$. From these gaussian distributions, we derive the sensitivities and obtain :

$$\delta(|\lambda_{\phi\phi}|) = 0.004 \quad \text{and} \quad \delta(\phi_{\phi\phi}) = 0.009 \text{ rad} \quad (83)$$

Interestingly, should the value of $\phi_{\phi\phi}$ be as large as 0.05, one would be able to exclude $\phi_{\phi\phi} = 0$ at the 5σ level, which would thus invalidate the Naive Factorization as well as the QCD Factorization, and would point towards physics beyond the SM.

We show in Fig. 7 the 1σ and 2σ contours in the plane $\phi_{\phi\phi}$ versus $|\lambda_{\phi\phi}|$ for the expected sensitivity at FCCee. Although it still remains to be studied in detail, we believe that the presence of the combinatorial background at the 10% level would not degrade these resolutions noticeably, thanks to the high statistics allowing one to study the background very precisely.

As mentioned, the overall fit enables also the determination of $\Delta\Gamma$. The sensitivity is :

$$\delta(\Delta\Gamma) = 0.004 \times 10^{12} s^{-1} \quad (84)$$

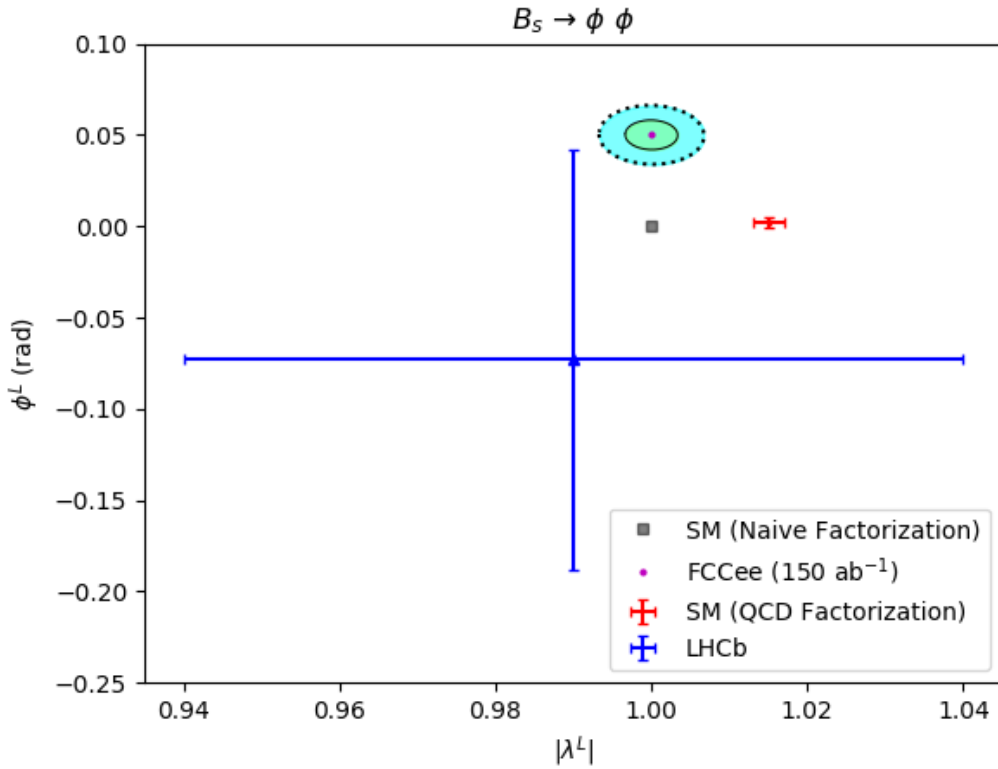


Fig. 7. Typical contour plot for the expected sensitivity on $\phi_{\phi\phi}$ versus $|\lambda_{\phi\phi}|$ at FCCee. The solid (dotted) ellipse curve is for 1σ (2σ). The input parameters are $|\lambda_{\phi\phi}| = 1$, $\delta(|\lambda_{\phi\phi}|) = 0.005$, $\phi_{\phi\phi} = 0.05$, $\delta(\phi_{\phi\phi}) = 0.01$, $\eta_{\phi\phi}^{eff} = 1 - 2f_{\perp} = 0.416$ and wrong tagging fraction $\omega = 0.25$. Are also shown the present sensitivity at LHCb and the expected SM theoretical values with NF or QCDF (56).

Finally, we wish to stress that the sensitivities in equation (83), in particular for $\phi_{\phi\phi}$ are not optimal as we did not carry out a full angular analysis. With such an angular analysis, one can expect to reduce further this error. Although one has to keep this possibility in mind, we do not assume such an improvement in the following of this paper, to remain on the conservative side. The study of this mode is particularly interesting for searching Beyond the SM physics and thus higher integrated luminosity would be most welcome either with higher instantaneous luminosity or enabling four interaction regions, or ideally both !

6.3 Constraints on FCC detectors

We explore the constraints relevant for this study that are to be considered when designing the detectors. To this end, we detail in Table 6 how the resolutions scale for the considered parameters.

Let us be more explicit on the experimental constraints.

Parameters	Errors scaling
$\phi_{\phi\phi}$	$\frac{1}{\eta_{\phi\phi}(1-2\omega)\sqrt{N}}$
$ \lambda_{\phi\phi} $	$\frac{1}{(1-2\omega)\sqrt{N}}$
$\Delta\Gamma$	$\frac{1}{\eta_{\phi\phi}\sqrt{N}}$

Table 6. The scaling of the errors for the various parameters determining the shape of the time dependent distributions for the decay mode $B_s(\bar{B}_s) \rightarrow \phi\phi$.

6.3.1 \sqrt{N} : Increasing the statistics

Several aspects are to be considered to increase the statistics :

- Increasing the instantaneous luminosity of the accelerator.
- Increasing the integrated luminosity, for example by operating 4 detectors and/or running more time at the Z-pole.

- Increasing the acceptance of the detector and the reconstruction efficiency. For the latter, one has to investigate the benefit of a large detection volume combined with a larger number of tracking points. This is particularly important since the K^+K^- tracks issued from each ϕ meson are very close to each other. A gaseous tracking detector (TPC or wire chambers) might be advantageous.
- An additional requirement concerns the overall tracking system resolution. Indeed, with an excellent momentum resolution, one is able to reduce the invariant B_s -mass resolution and hence reduce considerably the background. Not only point resolution is important but, maybe even more, very low material budget of the tracking system is of prime importance. Here again a gaseous tracking volume may be advantageous.

6.3.2 $(1 - 2\omega)$: decreasing the fraction of wrong tagging

In the present study, we have assumed conservatively $\omega = 25\%$ as it was achieved at LEP. Two main characteristics are important for reducing further the wrong tagging fraction:

- Excellent vertex resolution to identify the secondary and tertiary vertices, which are typical for the B decays. Such analysis is also mandatory to measure precisely the B_s flight distance. In this regard, a state-of-the-art pixelized vertex detector is unavoidable.
- Excellent overall Particle Identification to identify e^\pm , μ^\pm and K^\pm . For the latter particles, a Particle Identification system over a large range (at least up to ~ 25 GeV) is necessary. One may consider a specific PID system. However the wide momentum range makes this endeavour somewhat difficult. In particular, one has to ensure a minimal amount of material in front of the calorimeter to avoid degrading the energy resolution. An alternative is to use dE/dx , using cluster counting combined with an accurate Time of Flight system with a resolution of the order of 10 ps. A strong R&D program is thus necessary to assess experimentally what can be achieved in this area.

6.3.3 Disentangling the polarization states to maximize $\eta_{\phi\phi}$

As mentioned in this paper, averaging over the various polarization leads to an effective $\eta_{\phi\phi}$, which is +0.416 for $\phi\phi$. In order to improve further the experimental error, one needs to carry out a full angular analysis. This is also very interesting for the determination of

- The polarization fractions f_L , f_{\parallel} and f_{\perp} and confront them to QCD Factorization. As mentioned above, one can study CP violation ignoring the angular dependence. In that case, the measure CP violating angle $\phi_{\phi\phi}$ is reduced by the factor $\eta_{\phi\phi} = 1 - 2f_{\perp} = 0.416$. However, to be fully correct, this factor has to be corrected for the detector acceptance as it varies slightly according to the polarization states.
- The polarization dependent CP violating phases. Indeed these phases may be different for the various polarization and thus their determination would test with deeper detail the CP sector and eventually be sensitive to BSM physics.

6.4 Implication for New Physics in mixing

In the case of FCCee, one has instead of (71),

$$\frac{\text{Im}\Delta_s}{\text{Re}\Delta_s} \simeq 2\lambda^2\eta \text{Re}\left(\frac{a_c - a_u}{a_c}\right) + \phi_{\phi\phi}^{FCCee} = -\phi_{\phi\phi}^{SM} + \phi_{\phi\phi}^{FCCee} \quad (85)$$

If FCCee measures the CP phase of the SM within QCDF, i.e. the value (51), $\phi_{\phi\phi}^{SM} \simeq -2\lambda^2\eta \text{Re}\left(\frac{a_c - a_u}{a_c}\right) = -0.011$, then consistently one has $\text{Im}\Delta_s = 0$.

If we assume the central value found by LHCb (12,13) and the sensitivity $\delta(\phi_{\phi\phi}) = 0.01$, instead of the domain (80) in the case of LHCb, one would get from (85) the domain for NP in FCCee,

$$\frac{\text{Im}\Delta_s}{\text{Re}\Delta_s} = 0.011 - 0.073 \pm 0.010 = -0.062 \pm 0.010 \quad (86)$$

and to summarize one gets, with the assumed 1σ error,

$$-0.072 \leq \frac{\text{Im}\Delta_s}{\text{Re}\Delta_s} \leq -0.052 \quad (87)$$

In Fig. 8 this domain is compared to the one allowed by LHCb. This example shows that the sensitivity at FCCee would be efficient to put NP in evidence.

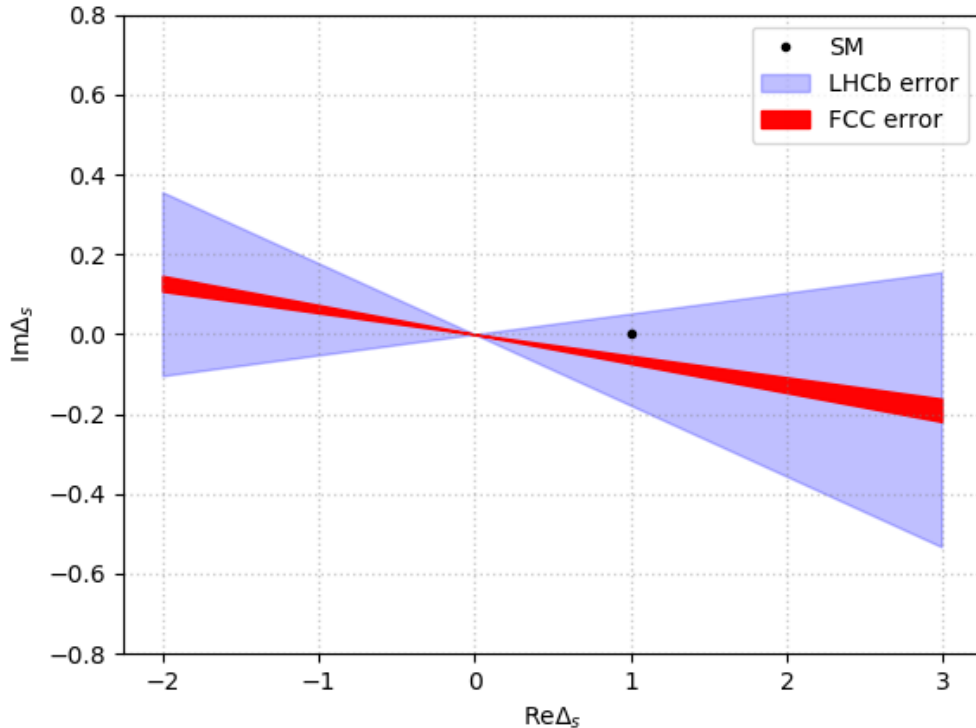


Fig. 8. The blue area shows the domain allowed in the plane $\text{Re}\Delta_s$ - $\text{Im}\Delta_s$ from the $B_s \rightarrow \phi\phi$ data at LHCb and the red area the expectation at FCCee with the central value of LHCb and the assumed uncertainty of Fig. 6 at 1σ . Taking into account the constraints from other observables [16], then only the domain for $\text{Re}\Delta_s > 0$ remains.

7 Coments on polarization-dependent rates and CP violation in QCDF

In this Section we summarize the main aspects of the calculation of the polarization fractions for the Penguin decay $\bar{B}_s \rightarrow \phi\phi$ in the QCDF scheme.

As argued in Section 2, owing to the hierarchies (4), and neglecting the amplitude $A(\bar{B}_s \rightarrow \phi\phi, h = +)$ as in (5), one expects the ordering (7), at odds with Table 1. We will see now how QCDF gives a much smaller longitudinal fraction.

Let us consider the ratio of transverse to longitudinal amplitudes,

$$R = \frac{A(\overline{B}_s \rightarrow \phi\phi, h = -)}{A(\overline{B}_s \rightarrow \phi\phi, h = 0)} \quad (88)$$

that gives, in the limit (5), the polarization fractions

$$f_L \simeq \frac{1}{1 + |R|^2}, \quad f_{\parallel} \simeq f_{\perp} \simeq \frac{|R|^2}{2(1 + |R|^2)} \quad (89)$$

From the notation (33), we get

$$R = \frac{\sum_{p=u,c} \lambda'_p S^{p,-} A_{\phi\phi}^- + (\lambda'_u + \lambda'_c) T^- B_{\phi\phi}^-}{\sum_{p=u,c} \lambda'_p S^{p,0} A_{\phi\phi}^0 + (\lambda'_u + \lambda'_c) T^0 B_{\phi\phi}^0} \quad (90)$$

where the CKM factors λ'_p are given by (34,35).

The coefficients for $h = 0$ of the direct diagram $A_{\phi\phi}^0$ and the annihilation diagram $B_{\phi\phi}^0$ are given by (36,37),

$$A_{\phi\phi}^0 = i \frac{G_F}{\sqrt{2}} m_{B_s}^2 A_0^{B_s \rightarrow \phi} (m_{\phi}^2) f_{\phi}, \quad B_{\phi\phi}^0 = i \frac{G_F}{\sqrt{2}} f_{B_s} f_{\phi} f_{\phi} \quad (91)$$

while the coefficients for $h = -$ of the direct diagram $A_{\phi\phi}^-$ and the annihilation diagram $B_{\phi\phi}^-$ are given by

$$A_{\phi\phi}^- = i \frac{G_F}{\sqrt{2}} m_{B_s} m_{\phi} F_-^{B_s \rightarrow \phi} (m_{\phi}^2) f_{\phi}, \quad B_{\phi\phi}^- = i \frac{G_F}{\sqrt{2}} f_{B_s} f_{\phi} f_{\phi} \quad (92)$$

The relevant combinations of the coefficients in QCDF for the $h = 0$ polarization are $S^{p,0}$ ($p = u, c$) and T^0 given by (40), T^0 being the annihilation.

In the paper we have chosen the $h = 0$ polarization and the corresponding CP violation, as made explicit in Section 4.2.

We need also the combinations of coefficients for the $h = -$ polarization, namely

$$\begin{aligned} S^{u,-} &= 2 \left(a_4^{u,-} + a_3^- + a_5^- - \frac{1}{2} (a_7^{u,-} + a_9^{u,-} + a_{10}^{u,-}) \right) \\ S^{c,-} &= 2 \left(a_4^{c,-} + a_3^- + a_5^- - \frac{1}{2} (a_7^{c,-} + a_9^{c,-} + a_{10}^{c,-}) \right) \\ T^- &= 2 \left(b_3^- + b_4^- - \frac{1}{2} (b_3^{EW,-} + b_4^{EW,-}) \right) \end{aligned} \quad (93)$$

For the calculation of the $h = -$ combinations (93) we use the very explicit formulas of Appendix A of ref. [3], that we compute for the $\overline{B}_s \rightarrow \phi\phi$ amplitude in our Appendix B.

Since the annihilation, as we will see, is crucial for the description of the polarization fractions, we use the model (2) of Table 3 for the $h = 0$ annihilation coefficients, computed in the Appendix C below, that includes the annihilation parameter

$$X_A = \left(1 + \rho_A e^{i\phi_A}\right) \ln \frac{m_{B_s}}{\Lambda_h} \quad (94)$$

consistently with the calculation of the annihilation amplitude for the transverse $h = -$ polarization.

For the sake of simplicity, and just to see for the moment the trend of the different effects, we use the central values of the parameters. In particular, we take for the annihilation parameters (94) the following values [3],

$$\rho_A = 0.6 , \quad \phi_A = -40^0 , \quad \Lambda_h = 0.5 \text{ GeV} \quad (95)$$

Below we will take into account the possible errors.

7.1 Remark on the form factors

Let us first make a remark on the form factors $A_0^{B_s \rightarrow \phi}$ and $F_-^{B_s \rightarrow \phi}$. In [3] the form factors used are consistent with the values from the QCD Sum Rules calculation of [23], that are somewhat different from the ones computed later in [22], and used in ref. [5] for the longitudinal amplitude. Both choices lead to different coefficients $A_{\phi\phi}^0$ and $A_{\phi\phi}^-$ in (91,92).

To see the trend of the effect of the form factors on the polarization fractions, we will perform the calculation of the ratio (90) for the two choices of the form factors used in [3] and [5], using for the moment the central values

$$(1) \quad A_0^{B_s \rightarrow \phi}(0) = 0.38 , \quad F_-^{B_s \rightarrow \phi}(0) = 0.65 \quad (96)$$

$$(2) \quad A_0^{B_s \rightarrow \phi}(0) = 0.47 , \quad F_-^{B_s \rightarrow \phi}(0) = 0.72 \quad (97)$$

The last number is obtained from [3]

$$F_-^{B_s \rightarrow \phi}(0) = \left(1 + \frac{m_\phi}{m_{B_s}}\right) A_1^{B_s \rightarrow \phi}(0) + \left(1 - \frac{m_\phi}{m_{B_s}}\right) V^{B_s \rightarrow \phi}(0) = 0.72 \quad (98)$$

where, to be consistent, we have used the values for $A_1^{B_s \rightarrow \phi}(0) = 0.31$ and $V^{B_s \rightarrow \phi}(0) = 0.43$ from the same sum rules calculation [22] giving $A_{\phi\phi}^0(0) = 0.47$, used in [5] and Table 2 for the longitudinal amplitude.

Let us remark that there is a sizeable difference for $A_0^{B_s \rightarrow \phi}(0)$ between both estimations (96) and (97).

For the two choices (1) and (2), (96,97), we get the coefficients $A_{\phi\phi}^0$ and $A_{\phi\phi}^-$ (91,92),

$$(1) \quad A_{\phi\phi}^0 = i \frac{G_F}{\sqrt{2}} \times (2.422 \text{ GeV}^3) , \quad A_{\phi\phi}^- = i \frac{G_F}{\sqrt{2}} \times (0.787 \text{ GeV}^3) \quad (99)$$

$$(2) \quad A_{\phi\phi}^0 = i \frac{G_F}{\sqrt{2}} \times (2.995 \text{ GeV}^3) , \quad A_{\phi\phi}^- = i \frac{G_F}{\sqrt{2}} \times (0.872 \text{ GeV}^3) \quad (100)$$

Let us split the complete calculation of the ratio (90) into different steps with different physical meaning in order to see their particular effect on the final result.

7.2 Limit of Naive Factorization

We observe first that the ratios of the coefficients of direct diagrams for $h = -$ with respect to $h = 0$ are given by

$$\left(\frac{A_{\phi\phi}^-}{A_{\phi\phi}^0} \right)^{(1)} = 0.325 , \quad \left(\frac{A_{\phi\phi}^-}{A_{\phi\phi}^0} \right)^{(2)} = 0.291 \quad (101)$$

respectively for the choices (1) and (2).

Therefore, at this step one would naively expect a much larger longitudinal polarization fraction than a transverse one.

In NF we take the limits $a_i^{c,h} = a_i^{u,h} \rightarrow C_i + \frac{C_{i\pm 1}}{N_c}$ (upper sign for i odd and lower sign for i even) and $b_i^h \rightarrow 0$. Then we find a longitudinal fraction

$$f_L^{NF} = \frac{|A_{\phi\phi}^0|^2}{|A_{\phi\phi}^0|^2 + |A_{\phi\phi}^-|^2} \quad (102)$$

that gives

$$\left(f_L^{NF} \right)^{(1)} \simeq 0.90 , \quad \left(f_L^{NF} \right)^{(2)} \simeq 0.92 \quad (103)$$

respectively for the choices (1) and (2).

7.3 Coefficients in QCDF for helicities $h = 0$ and $h = -$

In Tables 2 and 3 we have given the coefficients for the $h = 0$ amplitude. For the annihilation coefficients for $h = 0$ we will consider here Model (2), consistently with the annihilation in the $h = -$ amplitude that we give here below.

In Tables 7 and 8 we give the results of the QCDF coefficients for the $h = -$ amplitude, computed in Appendix B.

$a_3^- + a_5^-$	$a_4^{u,-}$	$a_4^{c,-}$	
$-0.005 - 0.001i$	$-0.047 - 0.015i$	$-0.046 - 0.001i$	
$(a_7^{u,-} + a_9^{u,-})/\alpha$	$(a_7^{c,-} + a_9^{c,-})/\alpha$	$a_{10}^{u,-}/\alpha$	$a_{10}^{c,-}/\alpha$
$0.68 - 0.03i$	$0.62 - 0.03i$	$0.29 + 0.17i$	$0.29 + 0.18i$

Table 7. Coefficients at NLO obtained in QCD Factorization for helicity $h = -$.

$r_A b_3^-$	$r_A b_4^-$	$r_A b_3^{EW,-}/\alpha$	$r_A b_4^{EW,-}/\alpha$
$-0.018+0.018 i$	-0.001	$0.022-0.028 i$	0.002

Table 8. Coefficients for $h = -$ annihilation, with $r_A = B_{\rho\rho}/A_{\rho\rho} = 5. \times 10^{-3}$, from $f_{B_d} = 0.200$ GeV, $f_\rho = 0.209$ GeV, $A_0^{B_d \rightarrow \rho}(0) = 0.30$ and $\alpha = 1/129$ [5].

We will use the coefficients of Tables 2 and 3 for $h = 0$ and Tables 7 and 8 for $h = -$ to compute the ratio $A(\overline{B}_s \rightarrow \phi\phi, h = -)/A(\overline{B}_s \rightarrow \phi\phi, h = 0)$ and therefore f_L . In order to clarify the origin of the enormous shift between the large naive value (103) and the final QCDF results and the data, we consider now different steps of the calculation.

Notice that we use universal values for both sets of form factors (96, 97). One must notice however, that the Hard scattering contributions depend on the form factors. We will however neglect small corrections coming from the difference of the form factors in these contributions.

7.4 Limit of neglecting Annihilation in QCD Factorization

To further clarify the origin of the final result for f_L we take the formal limit Annihilation $\rightarrow 0$ in the QCDF expression (90), and we find

$$\begin{aligned}
\left(\frac{|A(\overline{B}_s \rightarrow \phi\phi, h = -)|}{|A(\overline{B}_s \rightarrow \phi\phi, h = 0)|} \right)_{Ann \rightarrow 0}^{(1)} &= 0.606 \\
\left(\frac{|A(\overline{B}_s \rightarrow \phi\phi, h = -)|}{|A(\overline{B}_s \rightarrow \phi\phi, h = 0)|} \right)_{Ann \rightarrow 0}^{(2)} &= 0.526
\end{aligned} \tag{104}$$

for the choices of form factors (1) and (2), (96,97).

We realize that f_L decreases with respect to Naive Factorization, but still remains large,

$$(f_L)_{Ann \rightarrow 0}^{(1)} = 0.73, \quad (f_L)_{Ann \rightarrow 0}^{(2)} = 0.78 \quad (105)$$

for both choices of the form factors.

Moreover, it is important to emphasize that the parametrization (94) of the divergence in the annihilation plays an important role in the final result. Indeed, it is illustrative to compute the theoretical expression for f_L in the formal limit $\rho_A = 0$, i.e. for the default value $X_A = \ln \frac{m_{B_s}}{\Lambda_h}$

$$(f_L)_{\rho_A \rightarrow 0}^{(1)} = 0.81, \quad (f_L)_{\rho_A \rightarrow 0}^{(2)} = 0.68 \quad (106)$$

These values are much larger than experiment (Table 1), due to the cancellation $b_3^0 + b_4^0 \simeq 0$ (Table 3, Model (1)). One can also see in (106) the effect of the two choices of the form factors.

7.5 Final results in QCD Factorization

In the QCDF scheme, it is the Annihilation contribution that mostly changes the pattern of the polarization fractions. What happens is that the Annihilation for $h = -$ interferes constructively with the rest of the contributions. On the contrary, for $h = 0$ the annihilation amplitude has the opposite sign, and interferes destructively.

Taking all contributions into account, including Annihilation, our final result for the ratio of the moduli of $h = -$ and $h = 0$ amplitudes is

$$\left(\frac{|A(\overline{B}_s \rightarrow \phi\phi, h = -)|}{|A(\overline{B}_s \rightarrow \phi\phi, h = 0)|} \right)^{(1)} = 1.253, \quad \left(\frac{|A(\overline{B}_s \rightarrow \phi\phi, h = -)|}{|A(\overline{B}_s \rightarrow \phi\phi, h = 0)|} \right)^{(2)} = 1.086 \quad (107)$$

giving the polarization fractions

$$\begin{aligned} f_L^{(1)} &= 0.389, & f_{\parallel}^{(1)} &= f_{\perp}^{(1)} = 0.305 \\ f_L^{(2)} &= 0.456, & f_{\parallel}^{(2)} &= f_{\perp}^{(2)} = 0.272 \end{aligned} \quad (108)$$

for both choices of the form factors. The results for the choice (1) is in qualitative agreement with the experimental results of Table 1, while for the choice (2) the polarization fractions are somewhat off.

The BR of the decays into definite helicity vector mesons read,

$$BR(\bar{B} \rightarrow V_1 V_2, h) = S \frac{\tau_B}{8\pi m_B^2} |A(\bar{B} \rightarrow V_1 V_2, h)|^2 p \quad (109)$$

where $S = 1/2$ for identical particles, like in the case $B_s \rightarrow \phi\phi$, or $S = 1$ otherwise. Adding the rates for the $h = 0$ and $h = -$ polarizations, we find the total branching ratio,

$$BR(\bar{B}_s \rightarrow \phi\phi)^{(1)} = 24.8 \times 10^{-6}, \quad BR(\bar{B}_s \rightarrow \phi\phi)^{(2)} = 29.7 \times 10^{-6} \quad (110)$$

for both choices of the form factors. Choice (1) is in qualitative agreement with the experimental value of Table 1, and choice (2) gives a value that is too large. We will take into account errors on these quantities below.

In summary, the results (107-110) follow from the constructive interference of the Annihilation in the $h = -$ amplitude, and the destructive interference in the $h = 0$ one.

For completeness, we give here the CP violation parameters that we find for the different polarizations, using the notation (11) and the choice (1) of the form factors,

$$\begin{aligned} |\lambda_{\phi\phi}^{(L)}| &= 1.015, & \phi_{\phi\phi}^{(L)} &\simeq 10^{-3} \\ |\lambda_{\phi\phi}^{(\parallel)}| &= |\lambda_{\phi\phi}^{(\perp)}| = 1.004, & \phi_{\phi\phi}^{(\parallel)} &= \phi_{\phi\phi}^{(\perp)} \simeq 10^{-3} \end{aligned} \quad (111)$$

where the equalities between \parallel and \perp quantities follow from the motivated hypothesis (5).

7.6 Including errors in the calculation of the observables

For the sake of simplicity we have used the central values of the different parameters, giving the numerical results (108,110,111) for the observables.

We now take into account uncertainties on these parameters, given in Table 9. It is difficult to estimate the errors on the QCDF coefficients a_i^h , and we make the simple guess of a $\pm 10\%$ error. Concerning the annihilation, in both $h = 0, -$ amplitudes we adopt the errors on the parameters ρ_A, ϕ_A of ref. [3].

We restrict ourselves to the model (1) for the form factors, eq. (96).

We consider flat distributions around the central values of the parameters, with correlated guessed errors on the $a_i^h (h = 0, -)$. The errors are then added in quadrature and one gets the domains for the different observables of Figs. 9 - 12.

Parameter	Value
f_{B_s}	0.230 ± 0.005 GeV
f_ϕ	0.221 ± 0.005 GeV
$A_0^{B_s \rightarrow \phi}(0)$	0.38 ± 0.05
$F_-^{B_s \rightarrow \phi}(0)$	0.65 ± 0.06
a_i^0	$(1 \pm 0.10) \times$ Values of Table 2, Model (2)
a_i^-	$(1 \pm 0.10) \times$ Values of Table 7
ρ_A	0.6 ± 0.2
ϕ_A	$(-40 \pm 10)^0$

Table 9. Values and errors of the parameters. For the annihilation in both amplitudes $h = 0$, $h = -$, only large errors for the important parameters ρ_A and ϕ_A are considered.

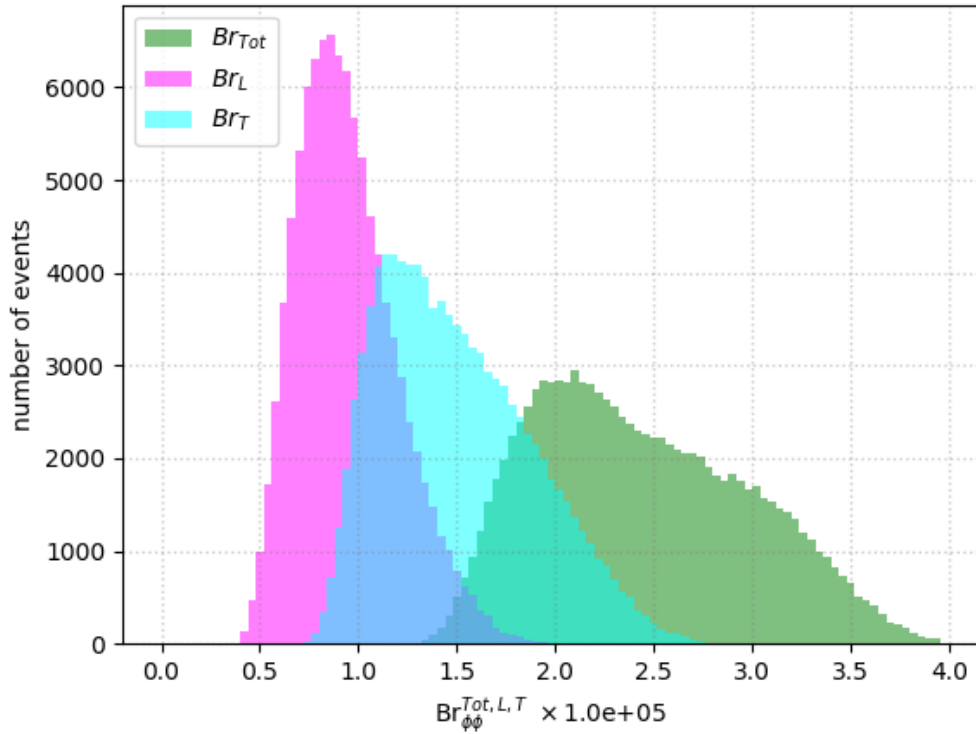


Fig. 9. L, T and total Branching Ratios with the input parameters of Table 9.

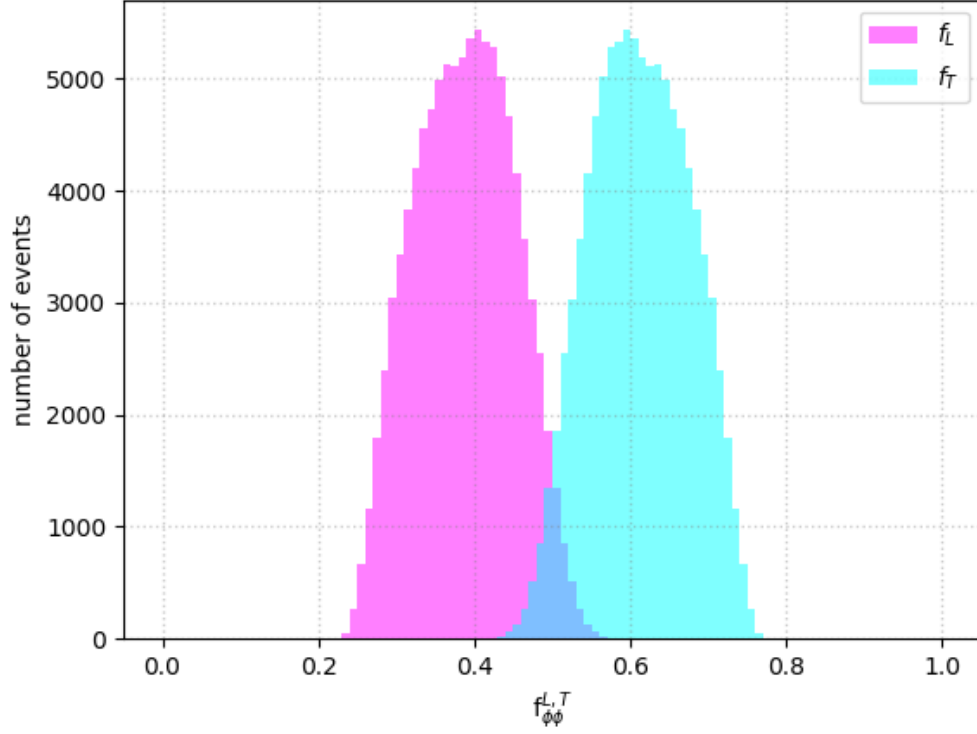


Fig. 10. L and T polarization fractions with the input parameters of Table 9.

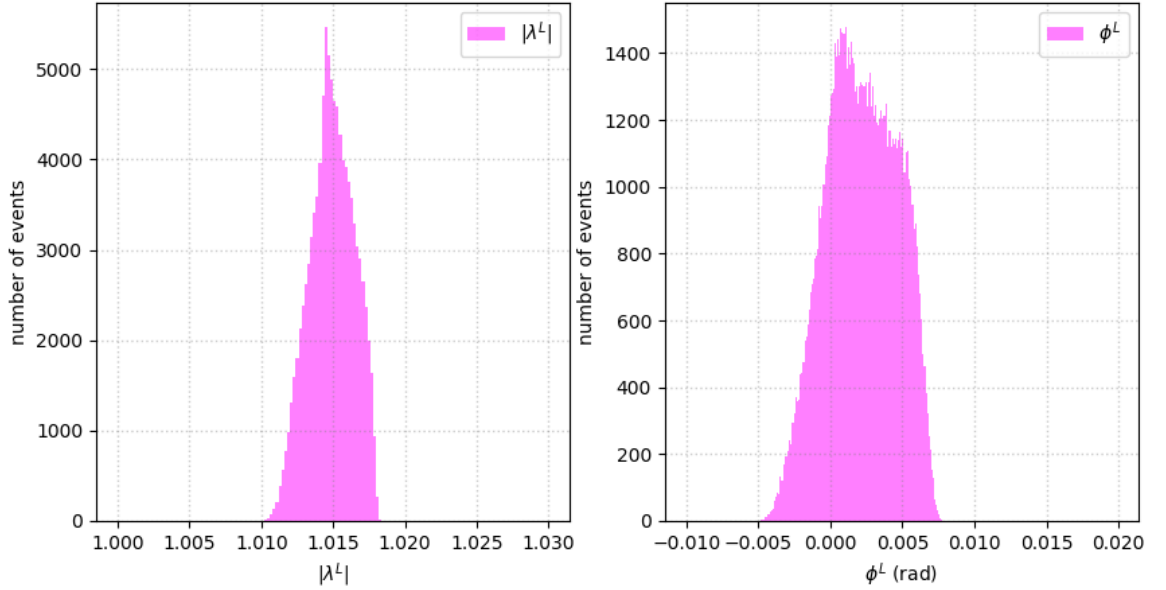


Fig. 11. Modulus and phase of the CP parameter $\lambda^L = \frac{q A(\bar{B}_s \rightarrow \phi\phi, L)}{p A(B_s \rightarrow \phi\phi, L)}$ with the input parameters of Table 9.

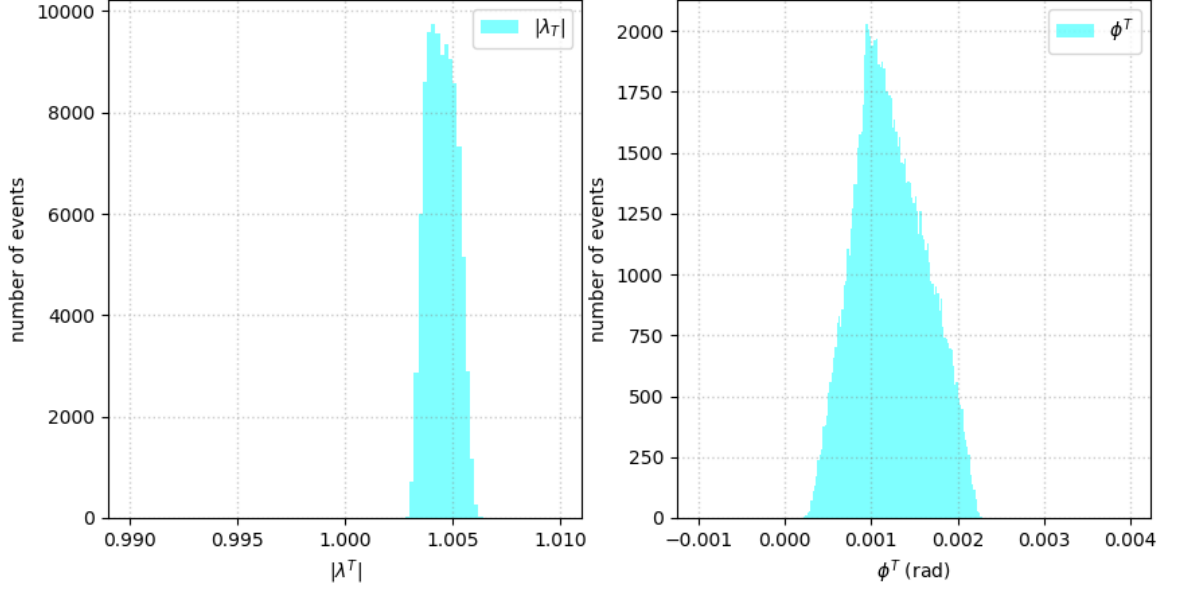


Fig. 12. Modulus and phase of the CP parameter $\lambda^T = \frac{q}{p} \frac{A(\overline{B}_s \rightarrow \phi\phi, T)}{A(B_s \rightarrow \phi\phi, T)}$ with the input parameters of Table 9.

The final result for the fitted observables is given in Table 10.

Observable	Result of the fit	Data
BR	$(2.44 \pm 0.63) \times 10^{-5}$	$(1.85 \pm 0.17) \times 10^{-5}$
BR_L	$(0.94 \pm 0.24) \times 10^{-5}$	$(0.70 \pm 0.02) \times 10^{-5}$
BR_T	$(1.50 \pm 0.41) \times 10^{-5}$	$(1.15 \pm 0.02) \times 10^{-5}$
f_L	0.39 ± 0.08	0.38 ± 0.01
f_T	0.61 ± 0.08	0.62 ± 0.01
$ \lambda^L $	1.015 ± 0.002	0.99 ± 0.05
ϕ^L	0.002 ± 0.003	-0.073 ± 0.115
$ \lambda^T $	1.005 ± 0.001	0.99 ± 0.05
ϕ^T	$0.001 \pm 4. \times 10^{-4}$	-0.073 ± 0.115

Table 10. Results of the fit for the observables of $\overline{B}_s \rightarrow \phi\phi$. The experimental CP violation parameters correspond to the polarization-independent fit of LHCb [1].

We observe that the branching ratios and polarization fractions are in agreement

with the data within 1σ , and the CP violation parameters are close to the Naive Factorization expectations.

On the other hand, since we have worked within the hypothesis that the amplitude A_+ vanishes (5), the transverse parallel and transverse perpendicular polarization fractions of the model are equal and given by

$$f_{\parallel} = f_{\perp} = 0.305 \pm 0.005 \quad (112)$$

consistently with the experimental value of Table 1,

$$f_{\perp} = 0.29 \pm 0.01 \quad (113)$$

7.7 The decay mode $\overline{B}_d \rightarrow \phi\phi$

Finally, let us remark that the decay mode $\overline{B}_d \rightarrow \phi\phi$, for which there is only an experimental upper bound, is very interesting since it follows uniquely from penguin annihilation [5] and could thus be a subtle test of the QCDF scheme. For this mode we find that the longitudinal amplitude dominates very much ($f_L \sim 99\%$) and we find a branching ratio $\sim (1.2 \pm 0.3) \times 10^{-8}$ consistent with the experimental limit $< 2.7 \times 10^{-8}$.

8 Caution remarks and conclusion

We have assumed NP contributions only for the mixing, as it is usually done. One should discuss however how possible NP in the Penguin diagrams could alter our results. There are a number of arguments pointing to dominance of a possible NP contribution in mixing. For example, assuming a new heavy W' boson, its contribution to the mixing will be quadratic in its mass, while it will be only logarithmic for the Penguin loop. But this deserves to be examined in more detail. The NP contributions in the Penguin decay amplitude are presumably small, but one can already say that, due to these contributions, the complex parameter Δ_s cannot be exactly the same for the mode $\overline{B}_s \rightarrow \phi\phi$ and for the standard mode $\overline{B}_s \rightarrow J/\psi\phi$.

It is important also to remark that, although both modes involve the same CP phase $-2\beta_s$ generated from the mixing, this phase is cancelled by $2\beta_s$ from the decay

in the mode $\phi\phi$, while it remains $-2\beta_s$ in the interference between mixing and decay in the mode $J/\psi\phi$.

On the theoretical side, we have restricted ourselves to the simpler case considered at LHCb [1], namely the time-dependent mixing induced CP violation, assuming that it is *the same* for the different polarization amplitudes, namely longitudinal, transverse parallel and transverse perpendicular. To estimate \bar{A}/A in the SM we have chosen the longitudinal polarization, on which very explicit results are given by [5] within the QCDF scheme, going thus beyond NF.

It would be necessary to have $\lambda_{\phi\phi}$ for the different polarizations L, \parallel, \perp in the QCDF scheme. We have performed this calculation along the lines of [3], obtaining the results of Table 10, approximately confirming that the LHCb polarization independent fit makes sense.

On the other hand, we have performed a calculation of the polarization fractions in the QCDF scheme for the penguin mode $\bar{B}_s \rightarrow \phi\phi$, and we have obtained theoretical values that turn out to be in agreement with experiment. We have traced the contradiction between the large Naive Factorization value for the longitudinal fraction f_L , close to $f_L \sim 0.90$, and the final much lower theoretical value within QCDF, closer to experiment, $f_L \sim 0.40$. We have paid special attention to the different contributions to f_L , and we have arrived to the conclusion that the annihilation for both the $h = 0$ and $h = -$ helicities is crucial in reproducing the data. We point out that the parametrization (94) of the weak annihilation IR-divergent quantity plays a crucial role in the final numerical result. One must keep in mind that this is a model-dependent quantity, and therefore the theoretical description of the polarization fractions largely relies on a model.

In conclusion, we have analyzed the pure Penguin mode to two vector mesons $\bar{B}_s \rightarrow \phi\phi$, that is experimentally clean and for which there are already measurements at LHCb. We have emphasized that in the interference quantity $\lambda_{\phi\phi} = \left(\frac{q}{p}\right)_{B_s} \frac{A(\bar{B}_s \rightarrow \phi\phi)}{A(B_s \rightarrow \phi\phi)}$, in the Naive Factorization limit the CP phase from the mixing exactly cancels the CP phase from the decay ratio. Therefore, this mode is suitable to distinguish possible NP in mixing. We estimate the deviation from the cancellation between the CP phases in mixing and decay by analyzing the ratio $\frac{A(\bar{B}_s \rightarrow \phi\phi)}{A(B_s \rightarrow \phi\phi)}$ beyond Naive Factorization, making use of the QCD Factorization scheme, that applies to

this case of two light mesons in the final state. We compare the theoretical value obtained for the modulus and phase of $\lambda_{\phi\phi}$ to the measurement at LHCb, and its implications for NP.

Finally, we make an estimation of the expected sensitivity at the future FCCee experiment for the CP phase and modulus of $\lambda_{\phi\phi}$. We find $\delta(|\lambda_{\phi\phi}|) = 0.004$ and $\delta(\phi_{\phi\phi}) = 0.009$ rad and, comparing to the LHCb data, we point out the implications at FCCee in the search of NP.

Appendix A. Wilson operators and short distance coefficients

The effective Lagrangian is given by

$$H = \frac{G_F}{\sqrt{2}} [V_{cs}^* V_{cb} (C_1 O_1 + C_2 O_2) - V_{ts}^* V_{tb} (C_3 O_3 + C_4 O_4 + C_5 O_5 + C_6 O_6)] + H_{EW}^{Penguin} \quad (114)$$

$$\begin{aligned} O_1 &= [\bar{c}\gamma^\mu(1 - \gamma_5)b] [\bar{s}\gamma_\mu(1 - \gamma_5)c] \\ O_2 &= [\bar{c}_\alpha\gamma^\mu(1 - \gamma_5)b_\beta] [\bar{s}_\beta\gamma_\mu(1 - \gamma_5)c_\alpha] \\ O_3 &= [\bar{s}\gamma^\mu(1 - \gamma_5)b] [\bar{q}\gamma_\mu(1 - \gamma_5)q] \\ O_4 &= [\bar{s}_\alpha\gamma^\mu(1 - \gamma_5)b_\beta] [\bar{q}_\beta\gamma_\mu(1 - \gamma_5)q_\alpha] \\ O_5 &= [\bar{s}\gamma^\mu(1 - \gamma_5)b] [\bar{q}\gamma_\mu(1 + \gamma_5)q] \\ O_6 &= [\bar{s}_\alpha\gamma^\mu(1 - \gamma_5)b_\beta] [\bar{q}_\beta\gamma_\mu(1 + \gamma_5)q_\alpha] \end{aligned} \quad (115)$$

where the Penguin contribution reads

$$H_{EW}^{Penguin} = -\frac{G_F}{\sqrt{2}} V_{ts}^* V_{tb} (c_7 O_7 + c_8 O_8 + c_9 O_9 + c_{10} O_{10}) \quad (116)$$

$$\begin{aligned} O_7 &= \frac{3}{2} [\bar{s}\gamma^\mu(1 - \gamma_5)b] [e_q \bar{q}\gamma_\mu(1 + \gamma_5)q] \\ O_8 &= \frac{3}{2} [\bar{s}_\alpha\gamma^\mu(1 - \gamma_5)b_\beta] [e_q \bar{q}_\beta\gamma_\mu(1 + \gamma_5)q_\alpha] \\ O_9 &= \frac{3}{2} [\bar{s}\gamma^\mu(1 - \gamma_5)b] [e_q \bar{q}\gamma_\mu(1 - \gamma_5)q] \\ O_{10} &= \frac{3}{2} [\bar{s}_\alpha\gamma^\mu(1 - \gamma_5)b_\beta] [e_q \bar{q}_\beta\gamma_\mu(1 - \gamma_5)q_\alpha] \end{aligned} \quad (117)$$

and the Wilson coefficients are given in Table 11.

C_1	C_2	C_3	C_4	C_5
1.086	-0.191	0.014	-0.035	0.010
C_6	C_7	C_8	C_9	C_{10}
-0.043	0.011 α	0.059 α	-1.229 α	0.246 α

Table 11. Wilson coefficients at NLO for $\mu = m_b = 4.2$ GeV in the NDR scheme.

Appendix B. The amplitude $A(\overline{B}_s \rightarrow \phi\phi, h = -)$

Here we make explicit some details of the calculation of the $h = -$ QCDF coefficients a_i^- and b_i^- summarized in Tables 9 and 10.

The coefficients a_i^-

From formulas (11) of [2] and (53) of [3] the coefficients $a_i^{p,-}$ ($p = u, c$) write

$$\begin{aligned}
a_i^{p,-} = & \left(C_i(\mu) + \frac{C_{i\pm 1}(\mu)}{N_c} \right) N_i^- + \frac{C_{i\pm 1}(\mu)}{N_c} \frac{C_F \alpha_s(\mu)}{4\pi} V_i^- \\
& + \frac{C_{i\pm 1}(\mu_h)}{N_c} \frac{C_F \alpha_s(\mu_h)}{4\pi} \frac{4\pi^2}{N_c} H_i^- + P_i^{p,-}
\end{aligned} \tag{118}$$

where we have made explicit that the scale is not the same for the Hard scattering term. The coupling α_s and the Wilson coefficients for both scales are given respectively by (120) and Tables 11 and 12.

Two scales μ and μ_h in QCDF

Let us make an important remark about the scales considered in QCDF.

The Wilson coefficients $C_i(\mu)$ relevant to the Vertex V and Penguin P contributions and the order $\alpha_s(\mu)$ NLO corrections specific to QCDF are estimated at some scale μ , that for definiteness we take to be $\mu = m_b = 4.2$ GeV.

For the Hard scattering H , due to off-shellness of the gluon in these diagrams [12], one adopts a *different scale* $\mu_h = \sqrt{\Lambda_h \mu}$ with $\Lambda_h = 0.5$ GeV and $\mu = m_b$, evaluating both at this scale the Wilson coefficients $C_i(\mu_h)$ and the coupling $\alpha_s(\mu_h)$

specific to the NLO corrections of QCDF. For the Annihilation corrections A one adopts the same Wilson coefficients $C_i(\mu_h)$ and coupling $\alpha_s(\mu_h)$.

This important point, that has sizeable quantitative consequences, has been put forward in refs. [3] and [5], following the earlier paper by Beneke and Neubert [15], who underline that both the running coupling constant and the Wilson coefficients for the Hard scattering and Annihilation terms have to be evaluated at an intermediate scale $\mu_h \sim \sqrt{\Lambda_{QCD} m_b}$ rather than $\mu \sim m_b$.

This different scale μ_h is much lower than μ , namely

$$\mu = m_b = 4.2 \text{ GeV} , \quad \Lambda_h = 0.5 \text{ GeV} , \quad \mu_h = \sqrt{\mu \Lambda_h} = 1.45 \text{ GeV} \quad (119)$$

This increases substantially $\alpha_s(\mu_h)$ and also the Wilson coefficients evaluated at this scale. One has

$$\alpha_s(4.2) = 0.224 , \quad \alpha_s(1.45) = 0.338 \quad (120)$$

and the Wilson coefficients at this latter scale are given in Table 12 (for the formalism see the detailed paper [24]).

C_1	C_2	C_3	C_4	C_5
1.190	-0.373	0.027	-0.062	0.012
C_6	C_7	C_8	C_9	C_{10}
-0.086	0.003 α	0.128 α	-1.353 α	0.430 α

Table 12. Wilson coefficients at NLO in the NDR scheme, at the scale $\mu_h = \sqrt{\mu \Lambda_h} = 1.45 \text{ GeV}$, relevant for the Hard scattering and Annihilation contributions.

Clearly, the Hard scattering and Annihilation diagrams will be very much enhanced due to the low scale μ_h .

Phenomenological parametrization of divergences

There are three divergences in QCDF, for which one adopts the phenomenological parametrizations of ref. [3], with $\Lambda_{QCD} = 0.225 \text{ GeV}$ and $\Lambda_h = 0.5 \text{ GeV}$,

$$X_H = \ln \left(\frac{m_{B_s}}{\Lambda_h} \right) , \quad X_A = \left(1 + 0.6 e^{-i40^\circ} \right) \ln \left(\frac{m_{B_s}}{\Lambda_h} \right) , \quad X_L = \frac{m_b}{\Lambda_{QCD}} \quad (121)$$

X_H enters in the Hard scattering, and X_A and X_L in the Annihilation contributions to the $h = -$ amplitude.

Normalization factors

$$N_i^-(\phi) = 0 \quad (i = 6, 8) , \quad N_i^-(\phi) = 1 \quad (i \neq 6, 8) \quad (122)$$

Vertex corrections

For $\mu = m_b$ one gets the simplified formulas

$$\begin{aligned} V_i^- &= \int_0^1 dy \phi_b(y) [-18 + g_T(y)] , & i \in \{1, 2, 3, 4, 9, 10\} \\ V_i^- &= \int_0^1 dy \phi_a(y) [6 - g_T(y)] , & i \in \{5, 7\} \\ V_i^- &= 0 , & i \in \{6, 8\} \end{aligned} \quad (123)$$

with

$$\begin{aligned} g_T(y) &= \frac{4 - 6y}{1 - y} \ln y - 3i\pi \\ &+ \left(2\text{Li}_2(y) - \ln^2 y + \frac{2 \ln y}{1 - y} - (3 + 2\pi i) \ln y - [y \rightarrow 1 - y] \right) \end{aligned} \quad (124)$$

Keeping only the lower twist, the distribution functions read

$$\Phi_V(v) = 6v(1 - v) \quad (125)$$

$$\phi_a(u) = \int_u^1 dv \frac{\Phi_V(v)}{v} = 3(1 - u)^2 , \quad \phi_b(u) = \int_0^u dv \frac{\Phi_V(v)}{1 - v} = 3u^2 \quad (126)$$

Numerically, one gets, for $\mu = m_b$,

$$\begin{aligned} V_i^-(\phi) &= -14 - 6i\pi , & i \in \{1, 2, 3, 4, 9, 10\} \\ V_i^-(\phi) &= 2 + 6i\pi , & i \in \{5, 7\} \\ V_i^-(\phi) &= 0 , & i \in \{6, 8\} \end{aligned} \quad (127)$$

Penguin corrections

Formulas (57)-(59) of [3] simplify for $\mu = \nu = m_b$,

$$\begin{aligned}
P_6^{-,p} &= P_8^{-,p} = 0 \quad (p = u, c) \\
P_4^{-,p} &= \frac{\alpha_s C_F}{4\pi N_c} \left\{ C_1 \left[\frac{2}{3} - G^-(s_p) \right] + C_3 \left[\frac{4}{3} - G^-(0) - G^-(1) \right] \right. \\
&\quad \left. + (C_4 + C_6) \left[-3G^-(0) - G^-(s_p) - G^-(1) \right] \right\} \quad (128) \\
P_7^{-,p} &= P_9^{-,p} = -\frac{\alpha}{3\pi} C_{7\gamma}^{eff} \frac{m_{B_s}^2}{m_\phi^2} + \frac{2\alpha}{27\pi} (C_1 + N_c C_2) \left[\delta_{pc} \ln \frac{m_c^2}{m_b^2} + 1 \right] \\
P_{10}^{-,p} &= \frac{\alpha}{9\pi N_c} (C_1 + N_c C_2) \left[\frac{2}{3} - G^-(s_p) \right]
\end{aligned}$$

The enhancement factor $\frac{m_{B_s}^2}{m_\phi^2}$ modifies the naive power counting in the EW penguins.

The function $G^-(s)$ reads

$$G^-(s) = \int_0^1 dy \phi_b(y) G(s - i\epsilon, 1 - y) \quad (129)$$

where $G(s, y)$ is the penguin function, formula (51) of [12],

$$G(s, x) = \frac{2(12s + 5x - 3x \ln s)}{9x} - \frac{4\sqrt{4s - x}(2s + x)}{3x^{3/2}} \arctan \sqrt{\frac{x}{4s - x}} \quad (130)$$

From $m_c = 1.3$ GeV, $m_b = 4.2$ GeV one has $s_c = 0.958$ and the values

$$G^-(0) = 2.333 + 2.094 i, \quad G^-(1) = 0.035, \quad G^-(s_c) = 2.090 + 0.315 i \quad (131)$$

From (131), and the value [12]

$$C_{7\gamma}^{eff}(m_b) = -0.318 \quad (132)$$

we find for the Penguin contributions at $\mu = m_b$,

$$\begin{aligned}
P_4^{-,u} &= -0.0086 - 0.0131i, & P_4^{-,c} &= -0.0067 + 0.0012i \\
P_7^{-,u} &= P_9^{-,u} = 0.0073, & P_7^{-,c} &= P_9^{-,c} = 0.0071 \\
P_{10}^{-,u} &= P_{10}^{-,c} = (-7. - 2.i) \times 10^{-5}
\end{aligned} \quad (133)$$

Hard scattering corrections

The Hard scattering corrections and the Weak annihilation contributions are estimated at the scale $\mu = \sqrt{m_b \Lambda_h} = 1.45$. The Hard scattering contributions H_i^- in (118) are given by the expressions

$$\begin{aligned}
 H_i^- &= -\frac{18 f_{B_s} f_\phi^\perp(\mu_h)}{m_{B_s} m_b F_-^{B_s \rightarrow \phi}(0)} \frac{m_b}{\lambda_{B_s}} (H_H - 1) , & i \in \{1, 2, 3, 4, 9, 10\} \\
 H_i^- &= \frac{18 f_{B_s} f_\phi^\perp(\mu_h)}{m_{B_s} m_b F_-^{B_s \rightarrow \phi}(0)} \frac{m_b}{\lambda_{B_s}} (H_H - 1) , & i \in \{5, 7\} \\
 H_i^- &= -\frac{9 f_{B_s} f_\phi}{m_{B_s} m_b F_-^{B_s \rightarrow \phi}(0)} \frac{m_b}{m_\phi \lambda_{B_s}} , & i \in \{6, 8\}
 \end{aligned} \tag{134}$$

Let us make a few remarks on these formulas.

The quantities H_i^- are a piece of the coefficients a_i^- (118) inversely proportional to the form factor $F_-^{B_s \rightarrow \phi}(0)$. Notice that this gives a form-factor dependence of the coefficients a_i^- , the rest of the terms in (118) being form factor independent.

The parameter f_ϕ^\perp is scale-dependent. At 1 GeV one has [5] $f_\phi^\perp(1\text{GeV}) = 0.186$ GeV, and we need this parameter at the scale $\mu_h = 1.45$ GeV,

$$f_\phi^\perp(\mu_h) = f_\phi^\perp(1\text{GeV}) \left(\frac{\alpha_s(\mu_h)}{\alpha_s(1\text{ GeV})} \right)^{C_F/\beta_0} = 0.179 \text{ GeV} \tag{135}$$

Finally, we take for the parameter $\lambda_{B_s} = 0.2$ GeV and H_H given by (121) [3].

Numerically one finds,

$$\begin{aligned}
 H_i^- &= -1.522 , & i \in \{1, 2, 3, 4, 9, 10\} \\
 H_i^- &= 1.488 , & i \in \{5, 7\} \\
 H_i^- &= -2.816 , & i \in \{6, 8\}
 \end{aligned} \tag{136}$$

Summary on the coefficients a_i^-

Gathering the precedent results in (118), and taking care of the two different scales $\mu = m_b$ and $\mu_h = \sqrt{\mu \Lambda_h}$ with $\Lambda_h = 0.5$ GeV for the different terms, one finds the coefficients a_i^- of Table 7.

The annihilation coefficients b_i^-

These coefficients are given by

$$\begin{aligned}
b_3^- &= \frac{C_F}{N_c^2} [C_3 A_1^{i-} + C_5 (A_3^{i-} + A_3^{f-}) + N_c C_6 A_3^{f-}] \\
b_4^- &= \frac{C_F}{N_c^2} [C_4 A_1^{i-} + C_6 A_2^{i-}] \\
b_3^{EW-} &= \frac{C_F}{N_c^2} [C_9 A_1^{i-} + C_7 (A_3^{i-} + A_3^{f-}) + N_c C_8 A_3^{f-}] \\
b_4^{EW-} &= \frac{C_F}{N_c^2} [C_{10} A_1^{i-} + C_8 A_2^{i-}]
\end{aligned} \tag{137}$$

with [3]

$$\begin{aligned}
A_1^{i-} = A_2^{i-} &= 18\pi\alpha_s \frac{m_\phi^2}{m_{B_s}^2} \left(\frac{1}{2} X_L + \frac{5}{2} - \frac{\pi^2}{3} \right) \\
A_3^{i-} &= 0 \\
A_3^{f-} &= 36\pi\alpha_s r_\perp^\phi (2X_A^2 - 5X_A + 3)
\end{aligned} \tag{138}$$

where the running of $r_\perp^\phi(\mu)$ is given by [5]

$$r_\perp^\phi(\mu) = \frac{2m_\phi f_\phi^\perp(\mu)}{m_b(\mu) f_\phi} = \frac{2m_\phi f_\phi^\perp(1\text{GeV})}{m_b(m_b) f_\phi} \left[\frac{\alpha_s(\mu)}{\alpha_s(m_b)} \right]^{-3C_F/\beta_0} \left[\frac{\alpha_s(\mu)}{\alpha_s(1\text{GeV})} \right]^{C_F/\beta_0} \tag{139}$$

and must be computed at the scale μ_h .

From $f_\phi^\perp(1\text{GeV}) = 0.186$ GeV [5] or $f_\phi^\perp(2\text{GeV}) = 0.175$ GeV [3], one finds consistently, for $\mu = \sqrt{m_b \Lambda_h} = 1.45$ GeV

$$r_\perp^\phi(1.45 \text{ GeV}) = 0.318 \tag{140}$$

and X_A and X_L are given by (121).

Numerically one finds,

$$A_1^{i-} = A_2^{i-} = 5.888, \quad A_3^{i-} = 0, \quad A_3^{f-} = 97.450 - 98.673i \tag{141}$$

and therefore,

$$\begin{aligned}
b_3^- &= -3.527 + 3.596i, & b_4^- &= -0.129 \\
b_3^{EW-} &= 0.034 - 0.044i, & b_4^{EW-} &= 0.004
\end{aligned} \tag{142}$$

that are given in Table 8, and one sees that the annihilation is largely dominated by b_3^- .

Appendix C. The annihilation contribution to the amplitude $A(\overline{B}_s \rightarrow \phi\phi, h = 0)$

For the longitudinal amplitude, the coefficients $b_3^0, b_4^0, b_3^{EW0}, b_4^{EW0}$ are given by the expressions (137) with $h = - \rightarrow h = 0$ and [5]

$$A_1^{i0} = A_2^{i0}, \quad A_3^{i0} = 0 \quad (143)$$

and

$$\begin{aligned} A_1^{i0} &\simeq 18\pi\alpha_s \left[\left(X_A - 4 + \frac{\pi^2}{3} \right) + (r_\perp^V)^2 (X_A - 2)^2 \right] \\ A_3^{f0} &\simeq -36\pi\alpha_s r_\perp^V (2X_A^2 - 5X_A + 2) \end{aligned} \quad (144)$$

With the parametrization

$$X_A = \int_0^1 \frac{dx}{x} = \left(1 + \rho_A e^{i\phi_A} \right) \ln \frac{m_B}{\Lambda_h} \quad (145)$$

and the values $\rho_A = 0.6, \phi_A = -40^0$ of ref. [3], one finds the annihilation coefficients for the longitudinal amplitude of Table 3 for model (2). One finds a very large coefficient b_3^0 , comparable in absolute magnitude to the transverse one b_3^- .

Acknowledgements

We are very much indebted to Martin Beneke and Gerhard Buchalla for providing us useful and detailed information on the QCD Factorization scheme applied to the decays of B mesons into two light vectors mesons.

References

- [1] LHCb Collaboration, R. Aaij et al., *Measurement of CP violation in the $B_s^0 \rightarrow \phi\phi$ decay and search for the $B^0 \rightarrow \phi\phi$ decay*, JHEP **12** (2019) 155, arXiv:1907.10003 [hep-ex].

- [2] A. Kagan, *Polarization in $B \rightarrow VV$ decays*, Phys. Lett. B **601** (2004) 151, arXiv:hep-ph/0405134.
- [3] M. Beneke, J. Rohrer and D. Yang, *Branching fractions, polarisation and asymmetries of $B \rightarrow VV$ decays*, Nucl. Phys. B **774** (2007) 64, hep-ph/0612290.
- [4] H.-Y. Cheng and K.-C. Yang, *Branching ratios and polarization in $B \rightarrow VV, VA, AA$ decays*, Phys. Rev. D **78** (2008) 094001, Phys. Rev. D **79** (2009) 039903 (erratum), arXiv:0805.0329.
- [5] M. Bartsch, G. Buchalla and C. Kraus, *$B \rightarrow V_L V_L$ Decays at NLO in QCD*, arXiv:0810.0249.
- [6] Belle Collaboration, K.-F. Chen et al., *Measurement of polarization and triple-product correlations in $B \rightarrow \phi K^*$ decays*, Phys. Rev. Lett. **94** (2005) 221804, arXiv:hep-ex/0503013.
- [7] BaBar Collaboration, B. Aubert et al., *Vector-tensor and vector-vector decay amplitude analysis of $B^0 \rightarrow \phi K^{*0}$* , Phys. Rev. Lett. **98** (2007) 051801, arXiv:hep-ex/0610073.
- [8] BaBar Collaboration, B. Aubert et al., *Observation of $B^0 \rightarrow K^{*0} \bar{K}^{*0}$ and search for $B^0 \rightarrow K^{*0} K^{*0}$* , Phys. Rev. Lett. **100** (2008) 081801, arXiv:0708.2248.
- [9] I. Dunietz, R. Fleischer and U. Nierste, *In Pursuit of New Physics with B_s Decays*, Phys. Rev. D **63** (2001) 114015, arXiv:hep-ph/0012219.
- [10] U. Nierste, *Three Lectures in Meson Mixing and CKM phenomenology*, Contribution to Helmholtz International Summer School on Heavy Quark Physics, arXiv:0904.1869.
- [11] G. Buchalla, A. Buras and M. Harlander, *The Anatomy of ϵ'/ϵ in the Standard Model*, Nucl. Phys. B **337** (1990) 313.
- [12] M. Beneke, G. Buchalla, M. Neubert and C. Sachrajda, *QCD factorization in $B \rightarrow \pi K, \pi\pi$ decays and extraction of Wolfenstein parameters*, Nucl. Phys. B **606** (2001) 245, arXiv:hep-ph/0104110.

- [13] M. Beneke, G. Buchalla, M. Neubert and C.T. Sachrajda, *QCD factorization for $B \rightarrow \pi\pi$ decays: Strong phases and CP violation in the heavy quark limit*, Phys. Rev. Lett. **83** (1999) 1914, arXiv:hep-ph/9905312.
- [14] M. Beneke, G. Buchalla, M. Neubert and C.T. Sachrajda, *QCD factorization for exclusive, nonleptonic B meson decays: General arguments and the case of heavy light final states*, Nucl. Phys. B **591** (2000) 313, arXiv:hep-ph/0006124.
- [15] M. Beneke and M. Neubert, Nucl. Phys. B **675**, (2003) 333, arXiv:hep-ph/0308039.
- [16] The CKMfitter Group, J. Charles et al., *Current status of the Standard Model CKM fit and constraints on $\Delta F = 2$ New Physics*, Phys. Rev. D **91** (2015) 7, 073007, arXiv:1501.05013 (2015).
- [17] P.A. Zyla et al. (Particle Data Group), Prog. Theor. Exp. Phys. 2020, 083C01 (2020).
- [18] M. Bicer, et al., First look at the physics case of TLEP, J. High Energy Phys. 01 (2014) 164, [https://doi.org/10.1007/JHEP01\(2014\)164](https://doi.org/10.1007/JHEP01(2014)164), arXiv:1308.6176.
- [19] A. Abada, et al., FCC Collaboration, Eur. Phys. J. C **79**(6) (2019) 474, <https://doi.org/10.1140/epjc/s10052-019-6904-3>.
- [20] A. Abada, et al., FCC Collaboration, Eur. Phys. J. ST **228**(2) (2019) 261, <https://doi.org/10.1140/epjst/e2019-900045-4>.
- [21] R. Aleksan, L. Oliver and E. Perez, Phys. Rev. D **105** (2022) 5, 053008, arXiv:2107.02002 [hep-ph].
- [22] P. Ball and R. Zwicky, *$B_{d,s} \rightarrow \rho, \omega, K^*, \phi$ decay form factors from light-cone sum rules revisited*, Phys. Rev. D **71** (2005) 014029, arXiv:hep-ph/0412079.
- [23] P. Ball and V. Braun, *Exclusive Semileptonic and Rare B-Meson Decays in QCD*, Phys. Rev. D **58** (1998) 094016, arXiv:hep-ph/9805422.
- [24] G. Buchalla, A. Buras and E. Lautenbacher, *Weak decays beyond leading logarithms*, Rev. Mod. Phys. **68** (1996) 1125, arXiv:hep-ph/9512380.